An Overview on Transport Phenomena within Solid Electrolyte Interphase and Their Impact on the Performance and Durability of Lithium-Ion Batteries

energies

MDPI

Review

An Overview on Transport Phenomena within Solid Electrolyte Interphase and Their Impact on the Performance and Durability of Lithium-Ion Batteries

Roberta Cappabianca [1], Paolo De Angelis [1], Matteo Fasano [1], Eliodoro Chiavazzo[1,*] and Pietro Asinari [1,2,*]

[1] Department of Energy "Galileo Ferraris", Politecnico di Torino, Corso Duca Degli Abruzzi 24, 10129 Torino, Italy; roberta.cappabianca@polito.it (R.C.); paolo.deangelis@polito.it (P.D.A.); matteo.fasano@polito.it (M.F.)

[2] Istituto Nazionale di Ricerca Metrologica, Strada Delle Cacce 91, 10135 Torino, Italy

* Correspondence: eliodoro.chiavazzo@polito.it (E.C.); pietro.asinari@polito.it (P.A.)

Abstract: The nature of the electrode–electrolyte interface has an impact on the performance and durability of lithium-ion batteries (LIBs). The initial electrolyte's thermodynamic instability at the anode–electrolyte interface in LIBs results in the formation of a passivation layer, called solid electrolyte interphase (SEI). The initial dense and intact layer allows Li^+ transport and restricts electron tunneling, thus preventing electrolyte decomposition and ensuring the electrochemical stability of a battery. However, the growth of this layer can reduce the availability of active lithium and electrolyte, and ultimately lead to an irreversible battery capacity fade. Investigating the transport phenomena of lithium ions within SEI is crucial for understanding its formation and growth. Nonetheless, accurately describing all relevant mechanisms is challenging due to its complex and multiscale nature. An overview of current computational efforts to study Li^+ transport within SEI is given in this article, ranging from electronic/atomistic scale simulations to macroscopic models. The drawbacks and advantages of the proposed numerical approaches are summarized along with the obstacles that need to be overcome to obtain accurate experimental data, identified on the basis of the most recent literature evidence. We highlight collaboration gaps between modeling and experimental approaches, as well as the urgent need for new multiscale models, to gain a better understanding of such a crucial transport phenomenon.

Keywords: diffusion; interface; lithium ion; battery; modeling

Citation: Cappabianca, R.; De Angelis, P.; Fasano, M.; Chiavazzo, E.; Asinari, P. An Overview on Transport Phenomena within Solid Electrolyte Interphase and Their Impact on the Performance and Durability of Lithium-Ion Batteries. *Energies* **2023**, *16*, 5003. https://doi.org/10.3390/en16135003

Academic Editor: Carlos Miguel Costa

Received: 18 May 2023
Revised: 14 June 2023
Accepted: 23 June 2023
Published: 28 June 2023

1. Introduction

Rechargeable or secondary batteries are devices that can convert chemical energy into electrical energy and vice versa for energy storage purposes. Secondary batteries have been used since the 1800s, but rechargeable lithium-ion batteries (LIBs) were not introduced until a century later [1]. In the 1900s, there was a technological revolution that resulted in the development of portable electronic devices such as video cameras, cell phones, and computers that required batteries with greater capacity or equal capacity with reduced size and weight. As a result, the search for a new rechargeable, small, and lightweight battery began, thus leading to the development of LIBs starting in the 1970s, with significant progress in the 1980s and 1990s [2]. At present, rechargeable batteries also play an important role in enabling the transition to a zero-emission society [3–5]. For example, electrochemical storage holds the promise to effectively cope with the intermittent nature of renewable energy technologies and their integration into energy grids [6]. LIBs continue to dominate the rechargeable battery market, but they are approaching their performance limits. Therefore, it is necessary to create the low-cost, high-performance, and long-lasting batteries of the future [7,8].

In their commercial implementations, lithium-ion batteries are typically composed of several electrochemical cells that are connected in series and/or parallel to provide the necessary voltage and capacity. Each cell consists of a positive electrode, a negative electrode, a separator, and an electrolyte solution [9]. Chemical reactions occur at the two electrodes, which are separated by a separator and immersed in an electrolyte solution. The separator serves as a physical barrier, preventing direct contact between the electrodes and thus reducing the risk of short circuits while allowing the transfer of lithium ions. The electrolyte solution acts as a transport medium for lithium ions between the electrodes. It contains a lithium salt that dissociates into lithium ions and other ions [10–12]. Figure 1 shows the operation of LIBs based on the reversible process of lithium-ion intercalation in the two electrodes. A popular option adopted for the positive electrode is lithium cobalt oxide ($LiCoO_2$). For the negative electrode, graphite is often used, with the electrolyte solution being a mixture of organic solvents. The main compound in the electrolyte is ethylene carbonate (EC), in which the lithium hexafluorophosphate ($LiPF_6$) salt is dissolved [13]. It is widely accepted that additional investigation into the chemistry and materials utilized in LIBs are necessary for the development of next-generation energy storage technologies [14,15]. This includes researching new materials for electrodes that can facilitate efficient lithium-ion insertion/extraction and exhibit higher theoretical capacities than conventional materials [16]. Moreover, researchers are exploring the incorporation of novel additives into electrolytes to enhance cycling performance, expand the temperature range of operation, and improve the electrochemical properties of the cells [17,18]. It has been observed that the current commercial electrolytes exhibit poor thermal tolerance and are prone to undesired decomposition and reactions with the electrode, mainly due to the highly reductive nature of EC. As a result, ongoing research endeavors aim to develop EC-free electrolytes to address these issues [19].

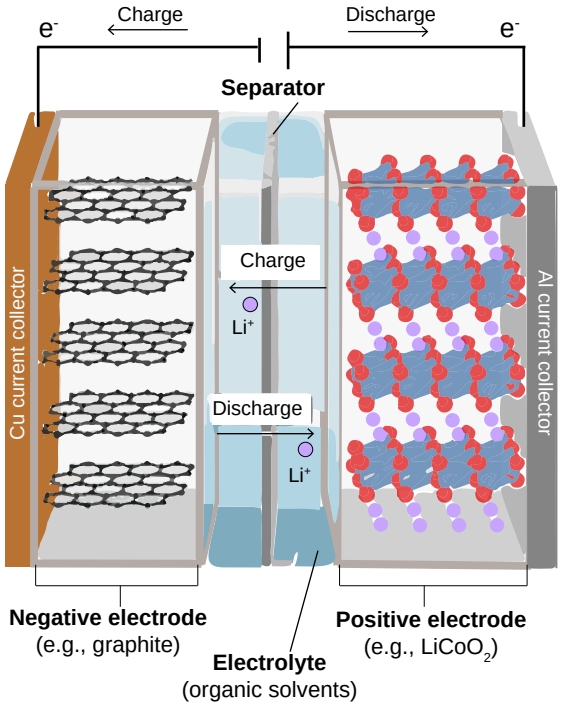

Figure 1. A lithium-ion battery's operation is shown schematically [20]. The negative electrode is composed of a low-potential material, such as graphite, whereas the positive electrode is composed of a transition metal that can release and receive lithium ions in its lattice. The electrolyte can be a liquid with a high ion conductivity and a wide potential window that is created by dissolving a lithium salt in an organic solvent.

The performance and lifespan of a battery are impacted by a multitude of factors, including cell design, charge/discharge rates, temperature, and more. To achieve optimal battery performance, it is crucial to consider these factors simultaneously. However, one particular aspect emerges as critically important in the development of high-performing batteries, i.e., the interfacial chemistry between the electrodes and the electrolyte. The characteristics of the electrode–electrolyte interaction play a significant role in determining the battery performance and represent a focal point for advancements in battery design [21–23]. The aging mechanisms of a LIB are:

1. The degradation of the battery's electrical components, such as corrosion of the current collector [24–26].
2. The change in the amount of lithium ions accessible for intercalation and deintercalation processes [24–26].
3. Structural changes in the active material (i.e., in the electrodes) and/or in the non-active material (i.e., in the separator and electrolyte) [24–26].

Such phenomena cause reversible or irreversible decreases in current density, capacity, and/or power. The formation of a passivation layer at the electrode–electrolyte interface is one of the most important irreversible phenomena occurring within LIBs [27]. This passivation layer forms as a result of the initial electrolyte's thermodynamics instability, which undergoes unwanted reactions during charge or discharge cycles at the anodic or cathodic interface, respectively [28]. Uncontrolled growth of this layer leads to degradation, whereas its initial formation is desirable for a battery's stability [29]. As a matter of fact, the initial dense and intact layer restricts electron tunneling and prevents the electrolyte from further reduction, which is essential for the chemical and electrochemical stability of a battery [30]. However, its excessive growth can deplete the active lithium and electrolyte, ultimately leading to an irreversible capacity fade of the battery. The choice of battery operation condition is relevant for the formation and growth of the passivation layer. Identifying an optimal charging strategy, for instance, can help avoid overgrowth or degradation of such layer [31]. In order to maximize battery performance and lifetime, greater attention is devoted to understanding the layer formed at the anode. This is due to the characteristics of the current anode materials because their higher reactivity and redox potential make the electrolyte more unstable on the anode side than on the cathode side. In addition, the anode material undergoes larger volume expansions than the cathode, which can induce mechanical stress at the interface [32,33]. Peled et al. [34] first defined this layer in 1979 as an electronically insulating and ionically conducting solid electrolyte interphase (SEI) between the anode and the electrolyte. Currently, there is no unanimous consensus regarding the terminology used to define this layer. Some studies refer to it as the solid electrolyte interface, such as Goodenough et al. [14], whereas others use the more-accurate term solid electrolyte interphase as defined by Peled et al. [35]. This discrepancy arises from the fact that the interphase is essentially a material found at the solid–liquid (or solid–solid in solid-state batteries) interface between the anode and the electrolyte [36]. Therefore, modelers commonly use the term "interface" to refer to the surface that separates two distinct domains, whereas materials scientists prefer the term "interphase" to indicate the actual material. To remove any ambiguity, in this work, we will adopt the term "interface" to denote the surface that separates the two phases and use the term "interphase" to refer to the material itself. The SEI is made up of inorganic and organic compounds. The inorganic component of the SEI is typically composed of lithium salts and their decomposition products, which can include lithium oxides, lithium carbonates, and lithium fluorides [37,38]. The organic component of the SEI is usually composed of polymeric materials, formed by the reduction of the electrolyte organic solvent, such as alkyl carbonates, vinylene carbonate, and various electrolyte solution additives [39,40]. The SEI components can be modified by adjusting the electrolyte content in the solution. For example, Figure 2 illustrates a comparison of SEI components discovered by Yun et al. [41] for two different mixture electrolytes on silicon negative electrode using a computational approach.

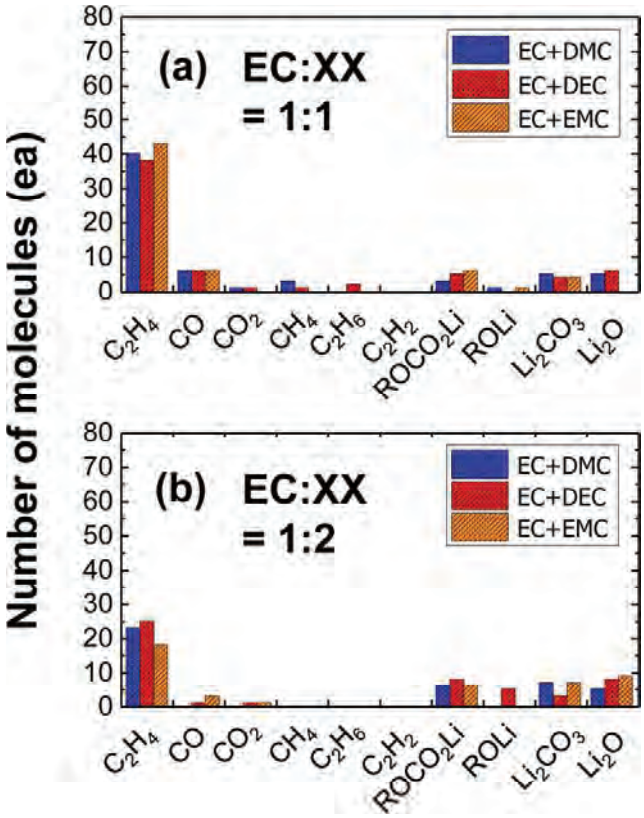

Figure 2. The SEI components revealed for the mixture electrolytes of: (**a**) EC/XX (XX = DMC, DEC, and EMC) = 1:1 and (**b**) EC/XX (XX = DMC, DEC, and EMC) = 1:2. They are gases (C_2H_4, CO, CO_2, CH_4, C_2H_6, and C_2H_2); inorganic (Li_2CO_3 and Li_2O); and organic components ($ROCO_2Li$ and ROLi: R = $-CH_3$ or $-C_2H_5$). This image is reprinted with permission from Yun et al. [41] (Copyright 2023 American Chemical Society).

SEI research has been ongoing for many years, with the goal of shedding light on its complex chemical structure and the mechanisms involved in its formation [32,42]. Nevertheless, SEI is one of the most important aspects of rechargeable batteries that is still poorly understood [43]. The scientific community is constantly looking for new strategies to design batteries capable of developing sufficiently stable SEI layer to reduce irreversible capacity loss and interface resistance. The goal is to create a dense, thin, and intact passivation layer that prevents further electrolyte reductions while also allowing lithium-ion (Li^+) transport [44]. Furthermore, it is essential to minimize the formation time of such layer due to its high cost and time-consuming nature. The formation steps involved in creating the SEI can take up to two or three weeks, resulting in a notable bottleneck in the LIBs production. Therefore, by accelerating the electrolyte wetting and SEI formation processes, considerable advantages in cost and production speed can be achieved [45,46]. Given that the reversible process of lithium-ion intercalation in the electrodes is a key aspect for the long-lasting LIBs, understanding lithium-ion transport phenomena in the SEI is extremely relevant and debated in the battery field [47,48]. The SEI's extreme chemical sensitivity to oxygen and hydrogen, as well as its complex chemical composition, limits experimental observation of this transport phenomenon [49–51]. In general, the thermodynamics and kinetic properties of the SEI layer cannot be characterized using current experimental techniques. Therefore, to overcome experimental constraints and study mass transport events in the SEI, a numerical approach based on physical models is required (see Figure 3). Furthermore, multiscale models including chemical reactions must be developed, ranging from the electronic to the continuum level, because the mechanisms of lithium-ion diffusion are characterized by disparate time and space scales [52–54].

The purpose of this review is to describe the various modeling approaches that have been suggested in the literature to date to shed light on the phenomenon of lithium-ion transport through SEI in LIBs. It will be stressed that although numerous studies have been conducted over the last forty years to understand the formation of SEI [55–58], the mechanism of lithium transport in SEI has only recently received more attention. As a result, we believe that it is important at this time to summarize and comment on the numerical methods reported in the literature to investigate the state-of-art research on such diffusive phenomenon. In particular, in the chapter entitled "Modeling of Li-ion diffusion", we will review the various computational studies that have been performed, categorizing them according to spatial and time scales, namely electronic, atomistic, mesoscale, and continuum. Furthermore, we will briefly discuss the experimental challenges associated with the mechanism of interest in the chapter entitled "Experimental measure of Li-ion diffusion". Finally, in the chapter entitled "Challenges and perspectives", we will critically analyze the knowledge gaps within the methods developed so far and indicate desirable future research paths in order to reach an adequate understanding of transport phenomena within SEI.

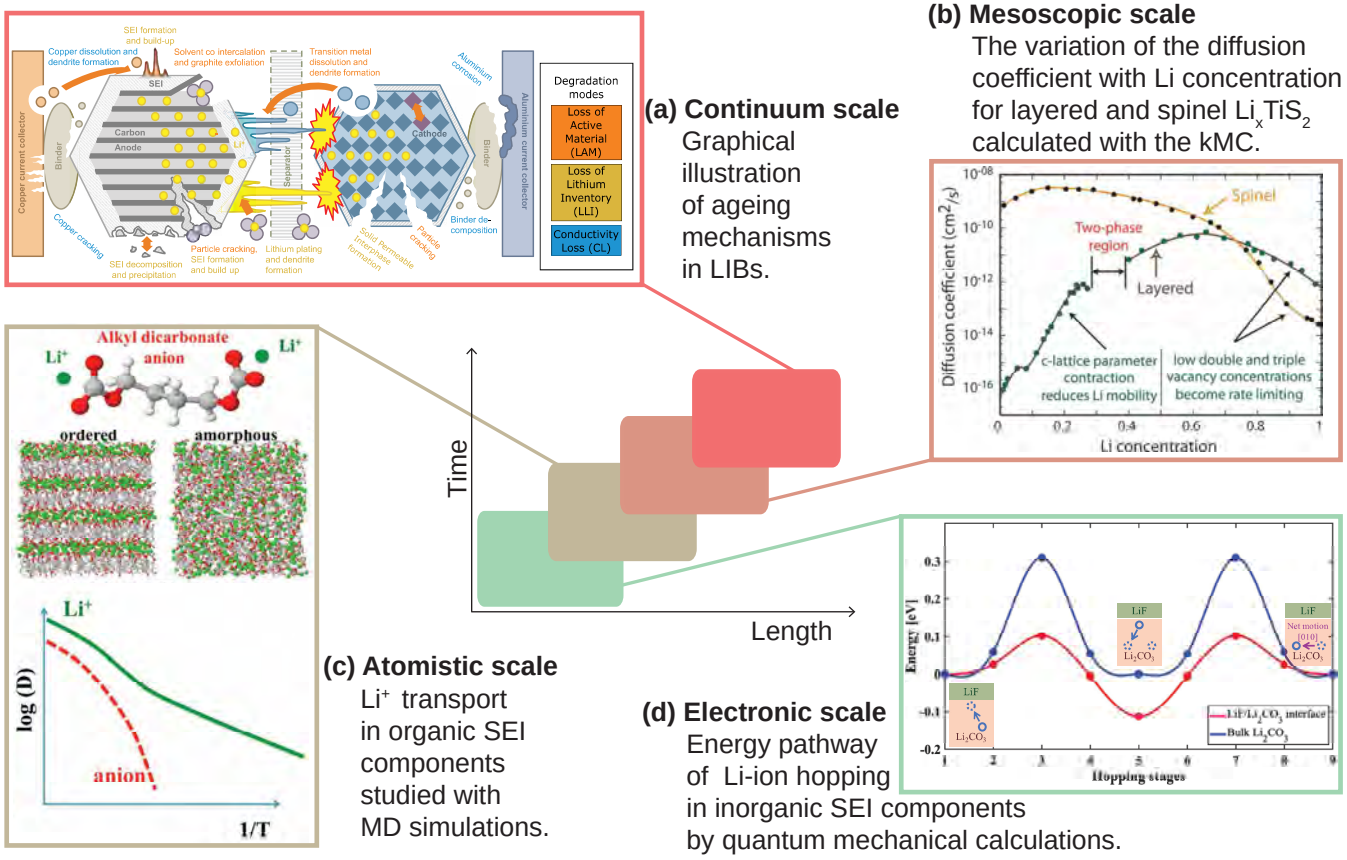

Figure 3. Overview of research methodologies using physical models and multiscale simulations. (**a**) Pastor-Fernández et al. [25] evaluated the merits of the techniques capable to identify and quantify aging mechanisms non-invasively (Copyright: Elsevier, under a license). (**b**) Van der Ven et al. [59] reviewed the key factors that govern Li^+ diffusion in electrode materials (reprinted with permission from Van der Ven et al. [59]. Copyright 2023 American Chemical Society). (**c**) Bedrov et al. [60] conducted an extensive investigation of structural, dynamic, and mechanical properties of organic SEI components using atomistic simulations (reprinted with the permission from Bedrov et al. [60]. Copyright 2023 American Chemical Society). (**d**) Ahmad et al. [48] probed the interface of inorganic SEI components to study its effects on electronic transport, Li-ion conduction, and defect formation using first principles (reprinted with permission from Ahmad et al. [48]. Copyright 2023 American Chemical Society).

2. Modeling of Li-Ion Diffusion

Lithium ions are the primary species that diffuse in a LIB due to their role as charge carriers in the electrochemical reactions during the charging and discharging processes. Other ions and species, such as additives or impurities such as water or metallic ions, may also diffuse to varying degrees depending on the specific battery design and chemistry [61]. Nevertheless, an efficient SEI, which is dense, thin, and intact has the advantage of limiting the transport of additives or impurities to the electrode, while allowing only the lithium ions to diffuse [62]. As a result, the ongoing research attempts to observe only the Li^+ diffusion mechanisms within SEI on very different spatial and temporal scales, as well as to determine how diffusion on the nano-scale and micro-scale affects the overall behavior of the battery.

Numerical models at the electronic scale can provide information on the various possible mechanism of lithium-ion diffusion, based on the characteristics and defects of the individual components of the SEI [63–65]. On the other hand, atomistic simulations can be used to determine the diffusion coefficient at the microscopic level [60,66,67]. Several mechanisms govern lithium mass diffusion, namely:

1. Interstitial diffusion occurs when lithium ions in interstitial positions in the crystal lattice move through interstitial sites or gaps between atoms.
2. Substitutional diffusion occurs when lithium ions replace other ions in the crystal lattice, resulting in the migration of Li ions within the lattice typically into vacant lattice sites. It is also known as the "knock-off" mechanism.
3. Vacancy diffusion can happen when a Li^+ moves into a vacant site, leaving a vacancy behind, and another lithium ion moves into the empty site, resulting in net lithium diffusion.
4. Hopping diffusion can occur when lithium ions jump from one lattice site to another through a series of intermediate sites, facilitated by thermal energy.

The specific mechanism or combination of mechanisms that dominate lithium diffusion depends on the material's crystal structure, temperature, and other external factors. Once this information on the nano-scale and micro-scale has been obtained, it must be determined how they can be incorporated into macro-scale models, to ensure that any micrometer-scale optimization of the transport processes has a quantitative impact on the battery performance estimated using continuum models.

Fick's laws are then used to calculate the flow of lithium ions in an LIB, where the diffusion coefficient must be known [68]. Hence, an ambitious goal could be to establish a clear relationship between microscopic and macroscopic diffusion rates. Meso-scale models are used to attempt to bridge the micro- and macro-scales. For example, once the possible diffusion paths of Li ions within a crystalline structure at the nano-scale have been determined, the kinetic Monte Carlo (kMC) method can simulate how the macroscopic diffusion rate varies as the concentration of Li ions changes by simultaneously considering all possible diffusion paths [59]. Energy barriers are needed as input parameters in the kMC method in order to calculate the rates of various diffusive events. These energy barriers represent the amount of energy required by diffusing species to move from one configuration to another. They are typically estimated using nano-scale models that calculate energy barriers for relevant diffusive events as the difference in energy between an initial and final configuration along a diffusive pathway. In this respect, the nudged elastic band (NEB) method or transition state theory (TST) can be used to estimate energy barriers for kMC simulations. Current numerical models are based on empirical assumptions that may not fully capture the complex behavior of the real LIB, especially under changing conditions or during different stages of battery operation. For instance, these assumptions include simplifications of the reactions at the electrode–electrolyte interface, such as using the empirical Tafel equation to calculate the reaction rate [52]. Furthermore, the battery materials are assumed to have idealized properties, such as uniform porosity or perfect conductivity, and lithium ions move uniformly through the electrolyte without taking into account factors such as diffusion barriers or interaction with other species [69,70]. As a

result, the ability to realize a multiscale model would allow for a reduction in empirical assumptions and the explicit description of the lithium-ion transport phenomenon.

2.1. Electronic Scale Models

Quantum chemical models based on electronic theories are often referred to as first-principles or ab initio techniques, and they play an important role in understanding the elementary reaction and transport processes within the main SEI components. The potential for accessing aspects of the electronic structure that are essential for analyzing its transport mechanisms is a major advantage of first-principles calculations. These theoretical models can explain the connections between structures and properties and allow for the investigation of mechanisms at the atomic scale and beyond. The ionic conductivity of SEI depends on the ion migration energy and the concentration of structural defects because the existence of point defects, such as vacancies and interstitials, causes ions to diffuse in solids [71]. In order to characterize the crystal structures formed in the SEI, their defects, the activation energy of the atomic hops, and more, first-principles calculations have been applied in numerous research activities [65,72,73].

Iddir et al. [74] conducted one of the first theoretical studies on lithium-ion diffusion in an inorganic SEI component using density functional theory (DFT) [75] calculations in 2010. They focused on the possible diffusion paths of the lithium ion within a lithium carbonate (Li_2CO_3) crystal, as this component is thought to be one of the most stable SEI components on the electrode surface [76]. First, they investigated the equilibrium position of an interstitial Li ion in the Li_2CO_3 crystal and then obtained the overall migration energy profile by applying the NEB [77] method to different diffusion paths. They were able to conclude from the results that the diffusion of the interstitial Li ion in Li_2CO_3 is almost two-dimensional, with migration favored along the [0 1 0] direction. Furthermore, the migration barrier calculated for Li-ion diffusion along the favored direction is about 0.28 eV, which is similar to the migration barrier calculated for lithium-ion diffusion in graphite (i.e., 0.3 eV under the lithium excess [78]). As a result, they were able to demonstrate that a thin layer of Li_2CO_3 on the graphite anode with the proper orientation can ensure good ionic conductivity without slowing down the transport of lithium ion in the graphite, while also improving electrolyte thermodynamics stability at the interface. Iddir et al. [74] focused on interstitial diffusion but, as Chen et al. [79] pointed out, Li ions also diffuse due to the presence of vacancies in the SEI crystal components. Hence, Chen et al. [79] used DFT to continue the investigation of Li-ion diffusion, this time attempting to shed light on the effect of vacancies in the crystal structures. Specifically, they investigated the diffusion of lithium ion into the main components of the inorganic SEI, namely the bulk of Li_2CO_3, lithium oxide (Li_2O), and lithium fluoride (LiF), by removing one lithium atom from the ideal supercell. Their findings demonstrated that the diffusion of Li^+ is accelerated by the existence of vacancies. In particular, their results showed a slight decrease in the energy barrier for Li^+ diffusion along the [0 1 0] plane in Li_2CO_3, thus reducing the previous value of approximately 0.28 eV for interstitial diffusion [74] to the values of 0.227 eV and 0.273 eV (see Figure 4i energy profiles (c) and (d)). Moreover, for lithium-ion diffusion along the [0 1 0] plane, a substantial decrease in the energy barrier was observed, ranging from the previously reported value of about 0.60 eV for interstitial diffusion [74] to the values of 0.491 eV, 0.267 eV, and 0.324 eV (see Figure 4i energy profiles (a), (b) and (e)). The energy barriers that Li ions must overcome to diffuse in Li_2CO_3 (see Figure 4i) and Li_2O (see Figure 4ii) are comparable to or slightly lower than those for Li ion diffusion in graphite, ranging from 0.308 to 0.400 eV [80], although they are greater in LiF (see Figure 4iii). As a consequence, a higher energy barrier for Li-ion diffusion in SEI than in graphite may be attributed to a higher concentration of LiF in the passivation layer.

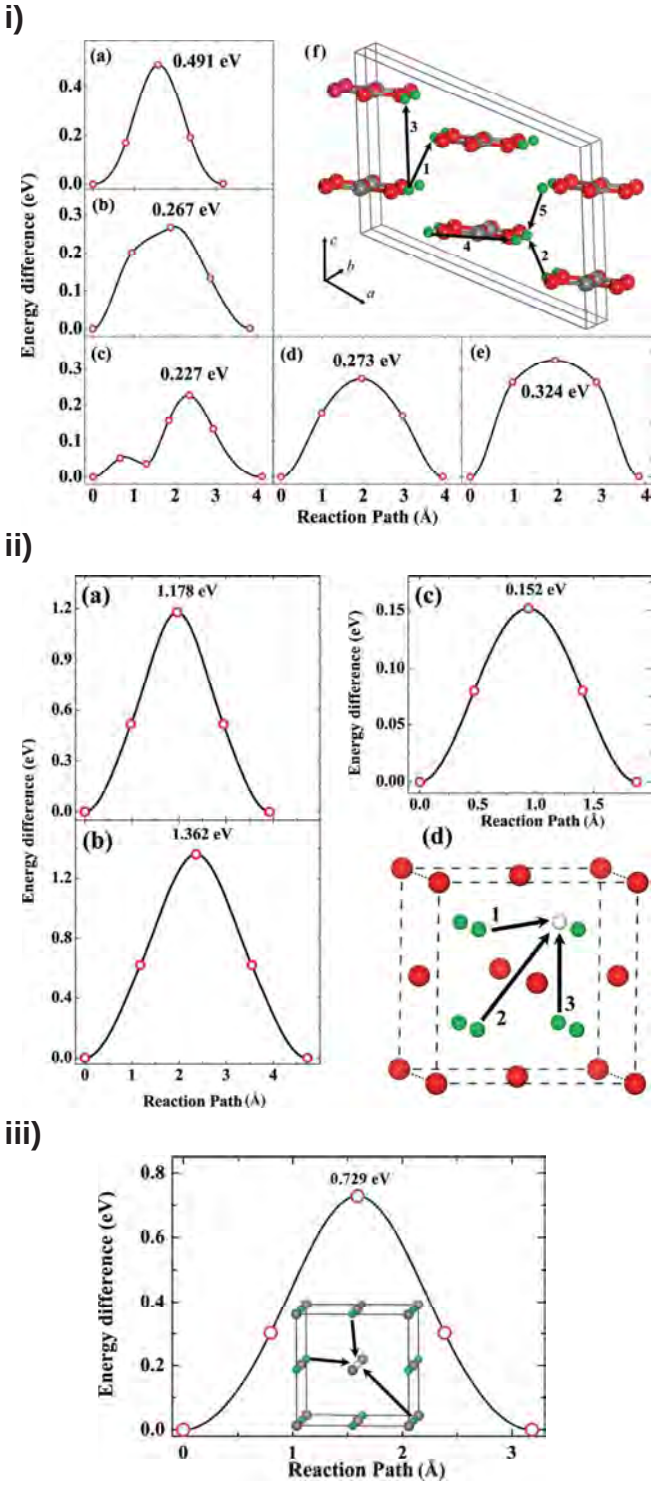

Figure 4. Possible Li-ion transport pathways in the SEI inorganic components using lithium vacancies (the position is indicated by a white sphere) and the corresponding energy barriers for lithium-ion diffusion along different pathways: (**i**) in Li_2CO_3, the energy profiles from (**a**–**e**) describe the diffusion of Li^+ along the 1–5 paths depicted in figure (**f**) (gray, red, and green spheres are C, O, and Li atoms, respectively); (**ii**) in Li_2O, Li-ion diffusion via the 1–3 path illustrated in figure (**d**) is defined by the energy profiles from (**a**–**c**), respectively, (red spheres are O and green spheres are Li); (**iii**) in LiF, the energy profile of a single Li-ion path (gray and green spheres are F and Li atoms, respectively). Reprinted with permission from Chen et al. [79] (Copyright 2023 American Chemical Society).

Nevertheless, as the SEI grows during battery operation, numerous defects and grain boundaries form, making the transport of Li ion to the electrode surface anisotropic and with changing paths. Ramasubramanian et al. [81] used DFT to understand and evaluate lithium-ion diffusion pathways through SEI grain boundaries. They identified grain boundaries between the inorganic SEI components that were mechanically and thermodynamically stable before running NEB calculations for a number of potential Li-ion diffusion paths. Their results revealed that the Li-ion diffusion rate was faster at the heterogeneous LiF/Li_2O grain boundaries than at the homogeneous LiF/LiF and Li_2O/Li_2O grain boundaries, as shown in Table 1. The lithium-ion diffusivity may differ from their estimates because the precise structure and arrangement of the grain boundaries in the SEI during battery operation can be hardly reconstructed. It is also worth mentioning the results found by Zheng et al. [82] using DFT calculations to investigate the transport of lithium ions within the inorganic components of the SEI in the same Table 1. It should be noted that the diffusion coefficients listed in Table 1 were calculated using the Arrhenius equation:

$$D = D_0 e^{-\frac{E_a}{k_B T}} \quad (1)$$

where E_a is the activation energy, k_B is the Boltzmann constant, and T is the temperature. The pre-exponential factor, D_0, is dependent on the dimensionality of the diffusion (1–3), the Li^+ migration distance (taken from the NEB path), and the lattice vibration frequency [47]. The values in Table 1 were calculated assuming a standard lattice vibration frequency of 10^{13} s^{-1}. However, this approximation may potentially alter the accuracy of the diffusion coefficient values. We observe some discrepancies in the activation energy values for the various Li^+ diffusion mechanisms within the SEI components by comparing results from the literature. For example, the E_a for lithium-ion diffusion in LiF driven by vacancies was equal to 0.729 eV in the work of Chen et al. [79], whereas Zheng et al. [82] reported a value of 0.66 eV. However, it appears that there is general consensus that the knock-off mechanism, in which an interstitial Li ion moves a crystalline structure atom, and the presence of defects (such as vacancies) are the fundamental aspects underpinning the diffusion of lithium-ion in inorganic SEI components.

Several environmental parameters, such as the applied electric field and temperature, have an impact on the transport of lithium ion in SEI as well. To evaluate these effects, various modeling approaches are frequently combined. The ab initio molecular dynamics (AIMD) [83] method is one way to research atomic-level diffusion mechanisms. Atomic interactions are derived from quantum mechanical calculations in this method, and then the atoms are allowed to propagate through the system according to the laws of classical mechanics. AIMD simulations can include systems of a few hundred atoms as well as short-lived phenomena lasting between 10 and 200 ps. For example, Ahmad et al. [48] used AIMD simulations to investigate the conduction of lithium ions at the interface of LiF and Li_2CO_3 as the temperature changed. Specifically, they studied the effects of this interface on Li-ion diffusion in Li_2CO_3. They compared their findings to those obtained for lithium-ion diffusion in the bulk and discovered a significant reduction in the activation barrier from 0.3 eV to 0.1 or 0.22 eV due to the interface (see Figure 5). Their work highlighted the importance of interfaces in the analysis of SEI properties.

Table 1. List of the computed lithium-ion transport properties through SEI grain boundaries [81] and within the inorganic components of the SEI [82] at room temperature estimated by electronic models. Figures representing the LiF/LiF, Li_2O/Li_2O, and LiF/Li_2O grain boundaries are reprinted with permission from Ramasubramanian et al. [81] (Copyright 2023 American Chemical Society), and figures showing LiF, Li_2CO_3, Li_2O, and LiOH crystal structure are used with permission of Royal Society of Chemistry from Zheng et al. [82] (permission conveyed through Copyright Clearance Center, Inc.).

Component		Li-Ion Diffusion Mechanism	E_a[eV]	D_0[m^2/s]	D[m^2/s]
LiF/LiF	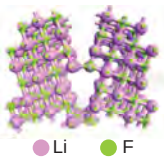	Through the grain boundary	0.68	$1.76 \cdot 10^{-6}$	$4.6 \cdot 10^{-16}$
Li_2O/Li_2O	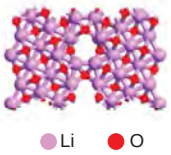	Through the grain boundary	0.78	$3.7 \cdot 10^{-6}$	$7.38 \cdot 10^{-16}$
LiF/Li_2O	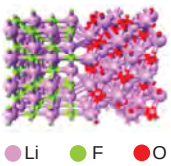	Through the grain boundary	0.45	$1.59 \cdot 10^{-6}$	$3.87 \cdot 10^{-14}$
Li_2CO_3	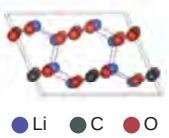	Vacancy	0.21	$5.308 \cdot 10^{-7}$	$1.649 \cdot 10^{-10}$
		Knock-off	0.24	$1.745 \cdot 10^{-6}$	$1.709 \cdot 10^{-10}$
		Direct-hopping	0.48	$2.516 \cdot 10^{-6}$	$2.415 \cdot 10^{-14}$
LiF	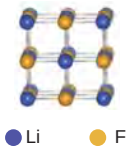	Vacancy	0.66	$2.438 \cdot 10^{-6}$	$2.305 \cdot 10^{-17}$
		Knock-off	0.25	$3.728 \cdot 10^{-6}$	$2.486 \cdot 10^{-10}$
		Direct-hopping	0.54	$1.242 \cdot 10^{-6}$	$1.187 \cdot 10^{-15}$
Li_2O	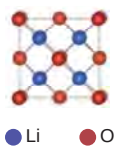	Vacancy	0.24	$1.624 \cdot 10^{-6}$	$1.591 \cdot 10^{-10}$
		Knock-off	0.49	$3.220 \cdot 10^{-6}$	$2.104 \cdot 10^{-14}$
		Direct-hopping	1.76	$3.220 \cdot 10^{-6}$	$1.287 \cdot 10^{-35}$
LiOH	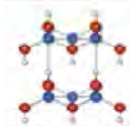	Vacancy	0.31	$9.400 \cdot 10^{-7}$	$6.238 \cdot 10^{-12}$
		Knock-off	0.20	$2.024 \cdot 10^{-6}$	$9.236 \cdot 10^{-10}$
		Direct-hopping	0.29	$1.272 \cdot 10^{-6}$	$1.821 \cdot 10^{-11}$

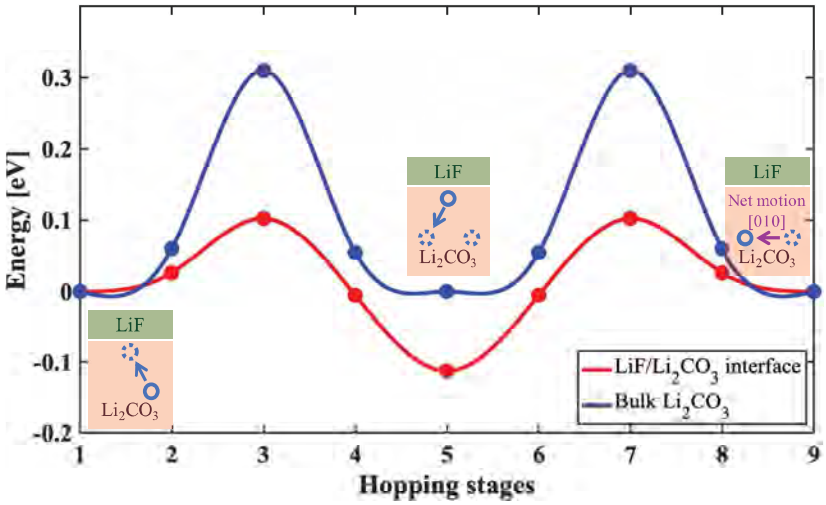

Figure 5. Energy profiles of interstitial lithium-ion motion in the Li_2CO_3: blue line refers to bulk and red line to a coherent interface with LiF. The knock-off diffusion mechanism is depicted in the interface under consideration. Interstitial lithium atoms are circled by a continuum blue line, whereas lattice lithium atoms that participate in the motion are circled by a dashed blue line. Reprinted with permission from Ahmad, et al. [48] (Copyright 2023 American Chemical Society).

2.2. Atomistic Scale Models

Molecular dynamics (MD) [84–86] simulations are atomistic simulations with a substantially lower computational cost than AIMD and electronic simulations. In MD, the electronic degrees of freedom are neglected in order to avoid the computational expense of calculating the electronic density. On the contrary, atomic interactions are typically calculated using the gradient of an effective potential energy surface $E(\mathbf{r})$, which is described as a sum of physically inspired interatomic interactions V. Each interaction is represented by a fixed shape function that depends only on the center of mass of the atom nuclei and the system topology $V = V(\mathbf{r}_i, \mathbf{r}_j, \dots)$. This collection of functions is referred to as a force field (FF). Over the past few decades, the need to model diverse atomistic systems has led to the development of several FFs formulations, which can be grouped into three main classes: classical FFs (sometimes also called Lennard-Jones FFs (LJFF)) [86], bond order-based FFs (BOFF) [87,88], and machine learning-based FF (MLFF) [89]. The LJFFs are the most widely used and numerically efficient FF in molecular dynamics simulations. This FF approximates the potential energy using bonded and non-bonded potentials. The bonded potential is typically described by mathematical functions that depend on the bond length, bond angle, and dihedral angle between atoms in a molecule. On the other hand, the non-bonded potential accounts for the van der Waals and Coulomb interactions between atoms and is a function of their relative distance, partial charge, and other electrostatic parameters. Usually, the LJFFs employ harmonic functions to describe the bond stretching, which effectively fixes the system topology during the simulation. However, this approach makes impossible the prediction of reactions within the system because it ignores key information about chemical bonding and reactions. As a result, it is unable to accurately describe reactive phenomena, such as bond breaking and formation. To address this limitation, the concept of bond order (BO) was introduced. Similar to its empirical analog introduced by Pauling [90], it is a continuum function representing the multiplicity of covalent bonds between atoms, which enables the connectivity of an atom to change dynamically during the system trajectory. Several force fields have been developed based on the BO concept, such as the reactive empirical bond order (REBO) [91], intermolecular reactive empirical bond order (AIREBO) [92], and Tersoff potentials [93], which can conveniently describe bond-breaking phenomena for specific systems. However, at present, the most used BOFF is the reactive force field (ReaxFF) proposed by Van Duin [94]. This potential incorporates

many-body functions that include classical and quantum mechanical effects, allowing it to predict bond dissociation more accurately. This ability to predict bond dissociation in chemical reactions is the primary reason behind the popularity of ReaxFF, making it one of the most widely used bond order force fields. Although BOFFs enable the prediction of various reactions and phenomena, their accuracy is still far from that of AIMD calculations [87]. In recent years, a more data-driven approach known as MLFF has been proposed. Instead of approximating the energy with a set of empirically inspired functional forms, MLFFs use descriptors (or kernels) and regressors or neural networks (NN) to interpolate the potential energy surface from ab initio calculations in a high-dimensionality space [89]. Although this approach loses the physical meaning of the coefficients calculated for the force fields, the resulting prediction accuracy is comparable to AIMD simulations [89]. For all the FFs mentioned above, the coefficients are usually computed using energy and forces from DFT simulations of a set of system configurations. The number of configurations required depends on the search space dimension for optimization, which is typically less than a hundred for LJFF, less than a thousand for BOFF, and more than a dozen of thousand for MLFF.

Transport properties on greater spatial and temporal scales can be determined by using classical MD instead of AIMD. In classical MD, force fields are further classified into two types: non-polarizable, where charges are fixed at the atomic centers [95,96], and polarizable, in which charges can move relative to the atomic centers [97–99]. Depending on the application, one must always evaluate the force field necessary for accurate molecular dynamics. The benefit of using MD simulations is that the potential diffusion paths do not need to be known beforehand, and the impacts of several particles can be taken into account. Benites et al. [67,100,101] used molecular dynamics simulations to investigate the main components of inorganic SEI. The diffusion coefficients of lithium ion were calculated over a temperature range of 250 K to 1800 K. They also investigated the effect of an applied electric field ranging from 0.1 V/Å to 0.85 V/Å. The diffusion coefficient was calculated using the lithium ion's mean square displacement (MSD) at each temperature [102]. Their findings on the dominant mechanisms for Li-ion diffusion in inorganic SEI were consistent with most of the previous theoretical results in the literature, namely knock-off and vacancy in LiF and Li_2CO_3, and interstitial in Li_2O.

In the literature, classical MD simulations have mainly been used to shed light on lithium-ion transport in organic SEI components. Di-lithium ethylene di-carbonate (Li_2EDC) is one of the main components that has been found experimentally in SEI organic [103,104]. In 2013, Borodin et al. [105] developed and used a many-body polarizable APPLE&P force field to investigate the ionic conductivity of the Li_2EDC component. They simulated the behavior of both the molten or disordered state and the crystal-like ordered state of Li_2EDC. Furthermore, they evaluated the impact of the many-body polarizable force field on the Li^+ diffusion in the molten state of Li_2EDC. On the one hand, they discovered that ordering slightly speeds up the lithium-ion transport in this SEI component. On the other hand, they found that the removal of polarization significantly slows down the lithium-ion diffusion phenomenon in the disordered Li_2EDC. Figure 6 displays their findings regarding the influence of ordering and polarizability on ionic transport. They obtained activation energy for lithium-ion transport in Li_2EDC in the range of about 0.663 eV to 0.871 eV, which is a bit higher than the activation energy of Li^+ in the graphite anode [106–108].

Later, Bedrov et al. [60] performed MD simulations to further investigate on the mechanism of lithium-ion diffusion in the amorphous and ordered states of organic SEI alkyl-carbonate compounds by using the same polarizable force field. They focused on analyzing how the properties of Li_2EDC and Li_2BDC changed with temperature. The diffusion coefficients of Li_2EDC and Li_2BDC were found to be similar at high temperatures, but as the temperature dropped, they discovered significant differences. For example, at 500 K the diffusion coefficient of Li_2EDC was approximately 20 times smaller than that of Li_2BDC. This comparison of the ordered and disordered states revealed that the

Li-ion diffusion in the ordered state is larger (see Figure 7a). The temperature range of ordered systems was 393–500 K, and the motion of Li^+ appeared to be primarily confined in 2D diffusion within the layers of the organic SEI components because they are close enough to allow occasional transfers of Li^+, as shown in Figure 7b. Slow SEI growth would give Li_2EDC enough time to form ordered structures, resulting in higher ionic conductivity. In contrast, despite its higher ionic conductivity, the presence of Li_2BDC in the SEI should be limited to optimize battery operation because they have a lower shear modulus (1.4 GPa compared to 2.8 GPa for Li_2EDC at 393 K) and reduce the SEI's ability to prevent dendrite growth.

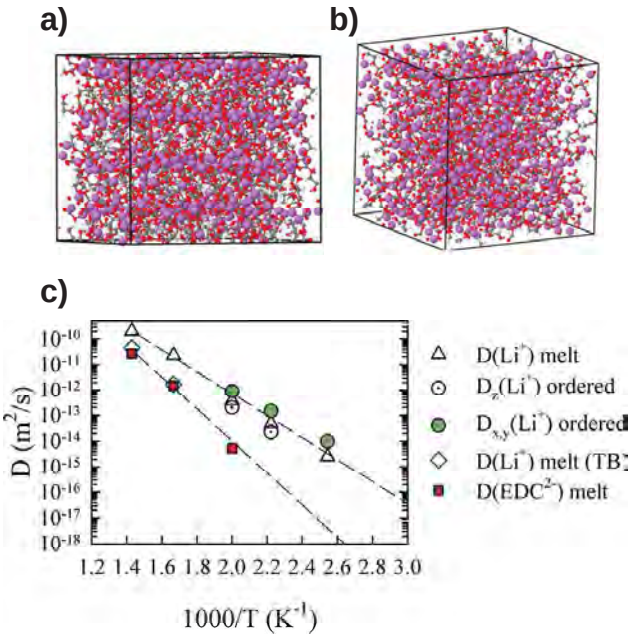

Figure 6. Snapshots from MD simulations at 450 K illustrate: (**a**) the ordered state and (**b**) the molten phase of Li_2EDC, where Li^+ are highlighted as pink balls. (**c**) The ionic diffusion coefficients in Li_2EDC are compared in two scenarios. Firstly, between the ordered and molten phases, both of which are simulated using a polarizable APPLE&P FF [109]. Secondly, between the molten phase simulated using the polarizable FF and the same phase simulated using a two-body FF (TB) with the polarization turned off. Reprinted with permission from Borodin, et al. [105] (Copyright 2023 American Chemical Society).

The following year, Muralidhran et al. [110,111] identified non-polarizable OPLS-AA force field parameters to examine lithium-ion transport properties in Li_2EDC. The structural information, such as the radial distribution functions, was in agreement with the results of the polarizable FF, indicating that their non-polarizable FF may be used to study the transport properties of Li_2EDC. Indeed, the diffusion coefficient of Li^+ in the amorphous Li_2EDC at a temperature of 333 K was found to be approximately $10^{-16} m^2/s$ in both MD simulations using polarizable and non-polarizable FFs.

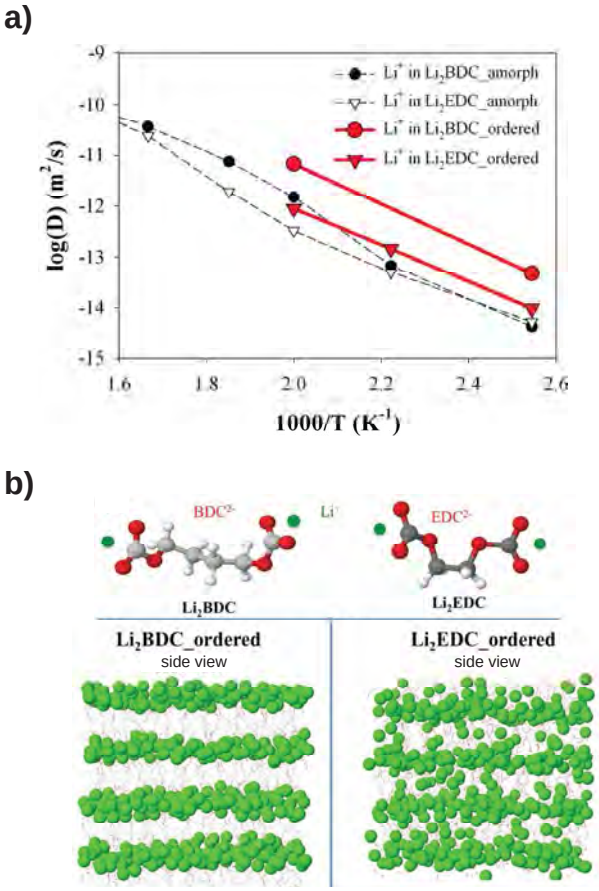

Figure 7. (**a**) Comparison of lithium-ion diffusion coefficients calculated using MD simulations in both the ordered and amorphous states of Li_2BDC and Li_2EDC components. The Li_2EDC results are reported in reference [105]. (**b**) Chemical structures of lithium alkyl dicarbonates are shown at the top, and the distribution of Li^+ in the ordered phases of Li_2BDC and Li_2EDC at 393 K is shown at the bottom. In the latter, the ions are shown as big spheres, and the counter-ions are shown as wire frames and transparent. Note that the spacing of layers in the ordered Li_2BDC is 10.0 Å and the spacing of layers in the ordered Li_2EDC is 8.0 Å. Reprinted with permission from Bedrov et al. [60] (Copyright 2023 American Chemical Society).

The reactive nature of lithium-ion batteries must be considered when studying the Li^+ transport phenomenon. As a result, reactive dynamics simulations, i.e., using a ReaxFF, should be performed rather than classical molecular dynamics simulations [112]. For instance, the reactive force field developed for Li-C-H-O atoms [113,114] was used to simulate the reduction of EC and dimethyl carbonate (DMC) solvents on a lithium metal surface [115]. The aforementioned works utilizing ReaxFF demonstrate the potential of this many-body force field in analyzing SEI properties. Nonetheless, it is important to note that the applicability of this potential is restricted to the available parametrizations in the literature, which have a limited scope of application [116]. Because the accuracy of ReaxFF depends heavily on the quality of the force field parameters, some of that can be obtained from experimental data when available, such as the equilibrium covalent bond and the dissociation energy, but the majority of them must be fine-tuned. One of the advantages of ReaxFF is that it uses fixed-shape functionals to approximate the potential energy surface. This allows for the use of a database that can be obtained with a limited number of ab initio calculations. For instance, when considering a couple of atom types, ReaxFF typically requires approximately 120–150 coefficients, depending on the number of angles and dihedral interactions to be included in the FF. Therefore, simulating around 300 well-designed configurations can provide enough data to calibrate these coefficients.

However, due to the strong nonlinearity of the equations used in the FF, only gradient-free optimization algorithms can be utilized, which can result in slow convergence. Additionally, the behavior of the resulting ReaxFF strongly depends on the region of phase space explored during the coefficient determination process. Therefore, using ReaxFF to study phenomena beyond the region explored during the ab initio calculations can lead to non-physical predictions [116]. In addition to the technical challenges of using ReaxFF, we must also consider some intrinsic issues in the formulation of the energy terms in the reactive force field developed by Van Duin. Originally developed in 2001 to model organic systems [94], the ReaxFF, over the past two decades, has undergone numerous modifications with the addition of new functional terms to enhance its applicability to a wider range of systems [87]. For example, a "lone-pair" energy term was introduced to improve the accuracy in hydrocarbon combustion [87,117,118], an improved three-body functional term was developed to handle $-NO_2$ group chemistry [87,119,120], and an energy term was included to account for hydrogen bonds in aqueous systems [117,121]. Therefore, the use of ReaxFF to predict the inorganic component of SEI may require a tailoring process of the energy terms in the FF, which necessitates a comprehensive understanding of the parametrization. This can limit the accessibility of this methodology to researchers outside the ReaxFF community. An alternative solution is to utilize MLFF to upscale AIMD data. Although this approach requires less knowledge about how the energy surface is interpolated, it necessitates an extensive ab initio simulation campaign to incorporate all potential configurations into the training set. Furthermore, reinforcement learning techniques [89] or the use of metadynamics may be necessary to explore the region in the phase space where the MLFF has high errors [122]. This process incurs significantly higher computational costs, even for simple systems, which is the main limit of why this new approach is not yet used in complex systems such as the anode–electrolyte interface. With the continued growth of computational power and the ongoing development of new and advanced machine learning techniques from the computer science community, it is realistic to think that soon it will be possible to describe SEI formation with the accuracy of MLFF, which is indeed is one of the main ambitious objectives of the European project BIG-MAP [8].

2.3. Bridging Micro- to Macro-Properties

In order to make meaningful comparisons between electronic/atomistic-level information and empirical observations on lithium-ion transport, it is crucial to upscale this information to larger time and space scales. The kinetic Monte Carlo [123] method is a valuable method for bridging the micro- and macro-scales [52,124]. This method is a Monte Carlo variant that allows dynamic simulations of stochastic processes. The time evolution of a system is tracked in the kMC simulations by probabilistically sampling rates of different events, such as particle hops or reactions, and updating the system state accordingly. The transition rates between different configurations of the system are typically calculated using the Boltzmann assumption [125]. According to the Boltzmann assumption, the transition rate (r) from a state A to a state B is proportional to the exponential of the negative energy difference between the two states divided by thermal energy, which is given by the product of the Boltzmann constant (k_B) and temperature (T). In the mathematical expression (Equation (2)), v_0 is the frequency of atomic vibration.

$$r(A \rightarrow B) = v_0 e^{-\frac{\Delta E}{k_B T}}. \quad (2)$$

Therefore, kMC can provide insight into the dynamic behavior of complex systems using information from the lower scale (such us ΔE), allowing for the study of diffusion, reactions, and other processes that are inherently random in nature. For example, Esmaeilpour et al. [126] developed a kMC protocol to elucidate the critical parameters governing the chemical, diffusion, and aggregation reactions that influence the formation

of an SEI with a thin inorganic component layer and a thick organic component layer (see Figure 8). This protocol leveraged nanoscale information obtained from first-principles calculations to learn about the ethylene carbonate reduction reactions at the graphite interface.

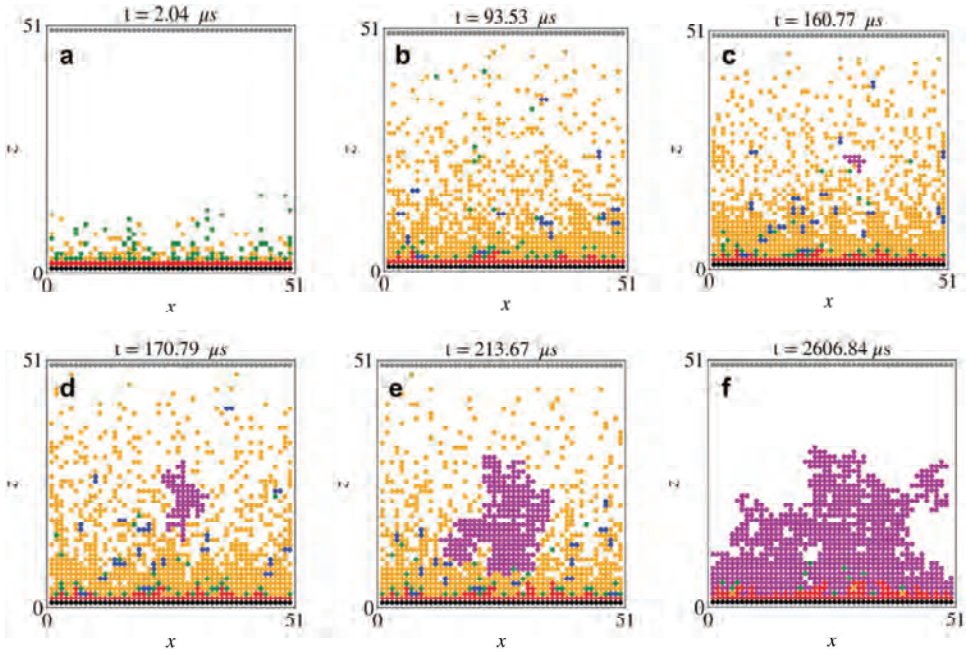

Figure 8. Different time instant snapshots of a 2D kMC simulation. At the start of the simulation, the graphite electrode is at the bottom and black in color, whereas all other sites are occupied by $EC - Li^+$. The intermediates and products of the reaction, i.e., Li_2CO_3, $C_2H_4OCOOLi$, Li_2EDC, $(Li_2EDC)_2$, and the organic SEI clusters, are represented by the red, green, orange, blue, and violet sites, respectively. The simulation evolution shows that: (**a**) $C_2H_4OCOOLi$ rapidly forms a stable inorganic SEI layer (Li_2CO_3), (**b**) Li_2EDC forms $(Li_2EDC)_2$, (**c**–**e**) organic SEI cluster begins to grow away from the electrode surface, and (**f**) organic SEI is deposited on the inorganic layer. Copyright 2023 Esmaeilpour et al. [126]. Advanced Energy Materials, under the terms of license.

One approach to determine ion transport properties in batteries is to perform first-principles calculations to extract activation energies for different diffusion paths, followed by kMC simulations to calculate diffusion coefficients numerically using stochastic ion migration simulations. For instance, Van der Ven et al. [59] used this strategy to determine the diffusion coefficient of lithium ions in electrode materials. They analyzed all conceivable pathways for lithium diffusion and used activation energy to determine their respective probabilities, utilizing first-principles calculations to gather the necessary information. Then, by performing a kMC simulation to identify the Li-ion diffusion pathway at each instant, they ensured a comprehensive sampling of the diffusion process and determined the lithium concentration dependence of the diffusion coefficient. In conclusion, their comprehensive first-principles statistical mechanical studies provided valuable insights for designing new electrode materials with a specific concentration dependence of the lithium-ion diffusion coefficient.

Continuum-scale mathematical models describe the transport of lithium ions in the SEI using macroscopic relationships of mass transport with physical parameters obtained from experiments or calculation at lower scales [127,128]. In particular, the model equations to describe the transport of the predominant specie in solids are Fick's laws, where J is the flux of lithium ions, c is the concentration, and D is the diffusion coefficient:

$$J = -D\nabla c \tag{3}$$

$$\frac{\partial c}{\partial t} = D\nabla^2 c. \quad (4)$$

The diffusion coefficient should be a known input parameter; however, approximations are often frequently used [129,130]. For example, in the capacity fading model for lithium-ion batteries of Ramadass et al. [131], the diffusion coefficient in the passivation layer was assumed to be the same as that in the graphite layer. Because this assumption is not totally true, it would be necessary to combine data collected at various spatial and temporal scales in order to accurately represent the transport phenomena in the SEI. Furthermore, according to Single et al. [132], the diffusion of interstitial lithium in the SEI could be the main mechanism involved in the long-term growth of this passivation layer. This conclusion would emphasize the importance of better understanding this transport phenomenon. Table 2 summarizes various computational studies, outlining the examined systems, utilized methods, and the computed properties relevant for gaining insights into the lithium-ion transport phenomenon.

Table 2. Summary of computational approaches on different spatial and temporal scales relevant to the investigation of lithium-ion transport within the SEI. It is noteworthy that, at the continuum scale, data on Li^+ diffusion in the SEI serve as valuable inputs for the model.

	System	**Method**	**Calculated Parameters**
Iddir et al. [74]	193 atoms (interstitial Li^+ added to the supercell of 192 atoms of Li_2CO_3)	DFT studies using NEB method for Li^+ diffusion	Energy barriers for Li^+ diffusion
Chen et al. [79]	64 atoms for LiF, 96 atoms for Li_2O and for Li_2CO_3	DFT studies using NEB method for Li^+ diffusion	Energy barriers for Li^+ diffusion
Ahmad et al. [48]	272 atoms (80 atoms of LiF and 192 atoms of Li_2CO_3)	NEB method and analysis of Car-Parrinello MD trajectories	Energy barriers and diffusion coefficient as a function of temperature (Arrhenius fit)
Bedrov et al. [60]	4096 atoms (256 Li_2EDC)	Analysis of MSDs of Li^+ obtained from MD simulations using polarizable APPLE&P FF	Diffusion coefficient as a function of temperature (Arrhenius fit)
Muralidhran et al. [110]	4096 atoms (256 Li_2EDC)	Analysis of MSDs of Li^+ obtained from MD simulations using non-polarizable OPLS-AA FF	Diffusion coefficient as a function of temperature (Arrhenius fit)
Van Der Ven et al. [59]	Layer and spinal crystal structure of electrode materials	kMC simulations to sample representative Li trajectories	Variation of the diffusion coefficients with Li concentration
Ramadass et al. [131]	Lithium-ion battery cell model	Diffusion coefficient is an input parameter of the mass transport equation	Capacity loss due to the side reaction over the negative electrode surface

3. Experimental Measure of Li-Ion Diffusion

The transport of lithium ions in the solid electrolyte interphase has an impact on the performance and safety of lithium-ion batteries. The ionic conductivity of the SEI layer can be affected by a variety of factors, some internal (composition and structure) and some external (temperature and voltage). Lithium-ion transport in this layer is primarily accomplished through a combination of diffusion, which is driven by the concentration gradient, and migration, which is driven by an electric field. In the existing LIBs, the SEI layer has lower ionic conductivity than the electrolyte. To improve the ionic transport properties of the passivation layer, the formation of this layer should be controlled to achieve the desired ionic conductivity [133,134]. However, the overview of the computational methods currently available in the literature has revealed gaps in the theoretical understanding of the lithium-ion transport phenomenon in the SEI [63,135–137]. As a result, the design of electrodes and electrolyte giving rise to a SEI with specific ion transport properties remains an unfulfilled challenge.

One of the main limitations of current computational models is that they are created to describe the behavior of a SEI with an ideal composition [138]. For example, electronic scale models have been used to investigate lithium-ion diffusion in ideal inorganic SEI components, which are far from the true complexity of inorganic SEI, in terms of defects, imperfections, grain boundaries, and other aspects [74,79,81]. Furthermore, atomistic scale models have focused on studying Li^+ diffusion in the main component of organic SEI (Li_2EDC), but the organic matrix of SEI is much more complex [60,105]. The SEI layer has a very complex chemical structure and composition, that is hard to identify experimentally due to its high sensitivity to oxygen and hydrogen. Another drawback of current numerical approaches is that they are not yet effective at bridging information across various spatial and temporal scales [139,140]. In other words, they are unable to connect data gathered at the atomistic scale with macroscopic observables such as loss capacity, voltage drop, etc. In this section, we provide a brief overview of some of the potential experimental approaches that could reveal useful information on lithium-ion transport in the SEI layer. There are several reasons for the lack of such experimental information. First and foremost, the difficulty of characterizing the structure and composition of SEI via experiment, as well as the challenge of observing its formation and growth in operando. For instance, the interpretation of Fourier-transform infrared spectroscopy (FTIR) and X-ray photo-electron spectroscopy (XPS) spectra is difficult and ambiguous because many SEI compounds are similar to one another and to the electrolyte. Furthermore, the chemistry of the SEI layer is sensitive to air exposure, which occurs frequently during sample transfer [141]. The use of other experimental techniques, such as transmission electron microscopy (TEM), is equally problematic due to the chemical reactivity and sensitivity of the SEI layer to electron beam irradiation [142]. As a result, the majority of experimental methods do not facilitate observation of the distribution and nanostructures of the organic and inorganic components in the SEI film. However, cryo-electron microscopy (cryo-EM) can be used to characterize the structure of SEI with atomic resolution [82]. There are no reactions at cryogenic temperatures, and structural and chemical information is preserved. For example, Figure 9 shows the Yuzhang et al.'s [51] observation of an SEI layer formed at the interface with a lithium metal electrode in (i) a standard electrolyte (i.e., ethylene carbonate-diethyl carbonate) and (ii) the electrolyte mixed with a fluorine-functionalized additive.

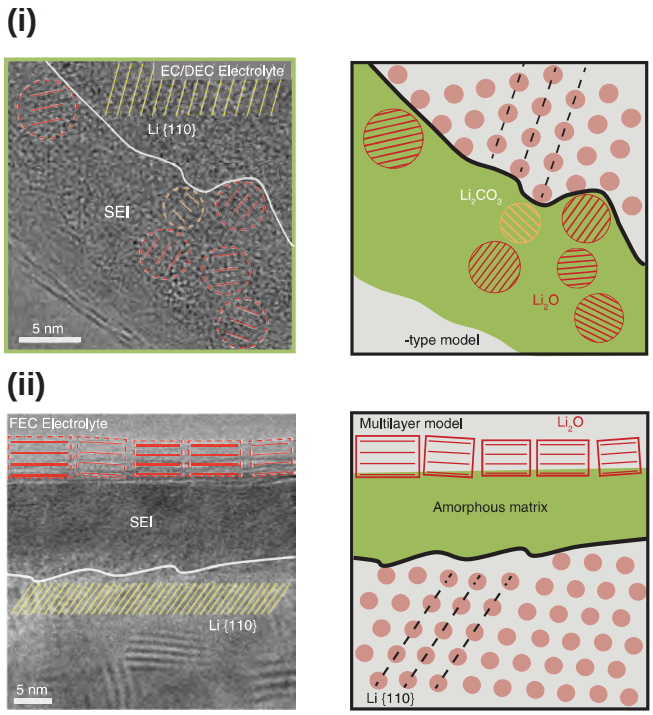

Figure 9. (**i**) The SEI formed in a standard electrolyte resembles a mosaic structure with a heterogeneous distribution of inorganic and organic components. (**ii**) The SEI formed in a carbonate-based electrolyte containing 10 % volume fluoroethylene carbonate appears to have a multilayer structure with an inner layer of amorphous polymer matrix and an outer layer of large grains of Li oxide. In both panels, the atomic-resolution images are on the left, and the schematics of the observed structure formed on Li metal are on the right. This figure is from Yuzhang et al. [51] and reprinted with permission from the American Association for the Advancement of Science.

To observe the diffusion of lithium ions in the SEI layer, a technique that investigates the crystalline structure of the SEI during the LIB's operating cycle is required. For example, a non-destructive tool that can be used to study the SEI layer is XPS with sputter depth profiles. By measuring the intensity of the emitted photo-electrons, the composition of the SEI can be determined. The sputter depth profiling technique enables the analysis of the SEI's thickness and its composition from surface to depth. This non-destructive approach allows for the characterization of the SEI's composition and thickness over time, but not its atomic structure [143]. Another non-destructive technique that can be used for determining the structure of the interface at the atomic scale is in situ synchrotron X-ray scattering. Chattapdhysy et al. [49] used this technique to investigate the formation and growth of a SEI layer on a graphene surface. Then, they examined the final structure and composition of SEI by using high-resolution transmission electron microscopy (HRTEM). Their results showed the formation of a LiF crystal that grows in quantity and size during lithiation, whereas the other SEI components remain amorphous because no additional crystals have been found. Amorphous material appeared to be present between the anode surface and the LiF crystal area according to the ex situ HRTEM in Figure 10. As a result, they concluded that crystalline LiF grows randomly in the organic components matrix rather than directly on the anode surface. This result may lead to the development of a novel numerical model for describing the lithium-ion transport in the SEI, specifically representing this layer as a mosaic structure composed of randomly distributed inorganic and organic components. This evidence is in contrast to most current numerical models in which the SEI is defined as a stratified state with an inner layer of inorganic material and an outer layer of organic material. Given the lack of enough experimental analyses, it is

unclear what the true final structure of SEI layer, whether mosaic or stratified, will be on the various anodic surfaces. Hence, additional experimental analyses are required in order to shed light on the lithium diffusion phenomenon in the SEI, but more importantly, close coordination and communication between the experimental and computational activity are needed.

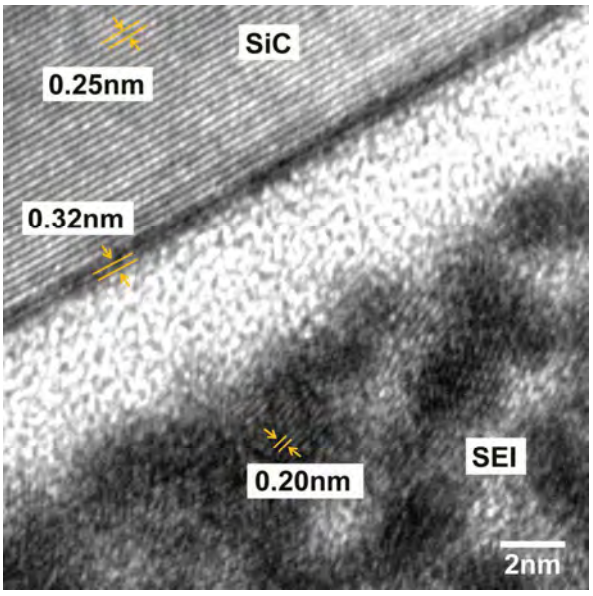

Figure 10. A representative ex situ HRTEM image of SEI at the graphene-coated SiC surface after 14 mA h cm^{-2} lithiation is shown. In the chosen orientation, the image reveals the crystal lattice structure of SiC (0001) with a layer spacing of 0.25 nm and 0.32 nm graphene spacing between the SiC and the SEI. Moreover, an area of roughly 3 nm thickness apparently amorphous between the graphene and LiF crystals is visible. LiF crystals, distant 0.20 nm, are randomly dispersed in additional seemingly amorphous regions. Reprinted with permission from Chattopadhyay, et al. [49] (Copyright 2023 American Chemical Society).

Synchroton-based operando measurements are costly, time-consuming, and frequently necessitate highly specialized geometries. Merrywaeather et al. [144] proposed the visualization of the dynamics of Li ions in the materials of the LIBs using the optical interferometric scattering microscopy technique (iSCAT). In particular, they focused on analyzing the lithiation and delithiation processes in single crystal particles of the cobalt oxide $LiCoO_2$, and discovered different crystal distortions during the two processes. Using phase-field modeling, they explained the distortions observed during lithiation and delithiation in terms of variations in the diffusion velocity of lithium ions in the crystal. This serves as another evidence of the potential for collaborations between cross-disciplinary modeling and experimental efforts. On the other hand, other measurable characteristics should be predicted by theoretical models for studying Li-ion transport in the SEI. Currently, after finding the diffusion coefficient experimentally, there are no relationships that allow it to be correlated with the knowledge attained at the electronic and atomic scales. As a result, we are unable to establish which lithium-ion diffusion mechanism, as well as which SEI structure and composition, influences the measured lithium diffusion coefficient. This last piece of information is critical for guiding the formation of SEI layer and achieving adequate ionic conductivity.

4. Challenges and Perspectives

Understanding the lithium-ion transport phenomenon in the SEI layer requires the development of new computational approaches based on physical models. To encourage cooperation between all the related research areas, it is also important to develop open, interoperable data infrastructures for LIB materials and interfaces [8,145,146]. In light of the recent increase in interest in investigating the Li-ion transport mechanism in the SEI, additional information from theoretical and experimental activities should be carefully collected and comparable figures of merit defined for model validation. In particular, the efforts of the scientific community should focus on the development of new multiscale models to investigate the lithium-ion transport mechanism in the SEI. Additionally, experiments that provide input parameters, such as the real chemical structure of SEI, and validate output information, such as capacity loss and voltage drop, should be used to enhance these models.

We believe that future computational efforts should focus on overcoming the three main critical issues encountered in this literature review, namely:

1. Investigating the diffusion of lithium ions in an SEI that is as realistic as possible, rather than just in the components of an ideal SEI that do not fully capture the complexity of the true SEI structure.
2. Employing a multiscale approach that transfers information from electronic/atomic scale to macro-scale, defined, bottom-up approach. This approach is advantageous for designing battery materials because it allows for a more comprehensive understanding of underlying physics and chemistry at each length scale. In contrast, a top-down approach relies more on empirical or phenomenological relationships and does not capture the full complexity of the system at each scale.
3. We also suggest the investigation "in vitro" and "in operando" of the SEI components to obtain a real measurement of the diffusion of Li atoms. These measures are crucial to validate all the past and future SEI models.

Concerning the first critical issue, the main challenge is to create an atomistic model of the SEI layer with morphology and composition as realistic as possible. To accomplish this, it would be necessary to run molecular dynamics simulations that faithfully reproduce the formation of the SEI components. Clearly, it is better to use reactive molecular dynamics instead of classical molecular dynamics to accurately simulate these reactive processes [41,147,148]. However, whenever the existing reactive FFs must be modified, the parametrization is computationally time-consuming and ineffective [149]. One possible solution could be to develop machine learning-based force fields [150]. The goal of this is to learn the statistical relationship between chemical structure and potential energy without prior knowledge of fixed chemical bonds or relevant interactions. The strength of these MLFFs lies in their ability to capture complex configurations and behaviors, limited only by the quality and quantity of training data [151–153]. Such MLFFs can utilize the knowledge gained from the training data to predict the behavior of unknown molecules more effectively than the reactive FFs that need to be customized for new systems. Although this new approach has yet to be extensively employed in complex systems such as the anode–electrolyte interface, we envision it as a tool that will enable an accurate description of SEI and its formation. Even if an appropriate force field is obtained, the SEI grows at different time and spatial scales than the initial formation of the layer; thus, it is challenging to simulate with MD. The main obstacle encountered when using MD to describe SEI evolution is the duration of the phenomenon, which is of the order of hours. To circumvent this problem, De Angelis et al. [154] developed a code that can build a SEI of a desired thickness by stochastically placing its inorganic components formed during the electrolyte's initial degradation at the electrode interface. A tool such as this enables a subsequent simulation in which the first layer of inorganic SEI is already at the electrode interface and the subsequent growth of SEI is investigated, thereby shortening the overall duration of the phenomenon. Therefore, we believe that this code could enable the study of the lithium-ion transport phenomenon in a passivation layer that is as realistic

as possible (inspired by the Peled et al. hypothesis [35]), rather than only in the individual ideal components of the SEI.

In regard to the second critical issue, communication between molecular-scale and continuum models is crucial for understanding lithium-ion transport in the heterogeneous SEI structure and allowing comparisons with experimental observables [155,156]. To fill the gap between molecular and continuum scales, mesoscale models, such as the kinetic Monte Carlo model, are frequently used. To date, they have primarily been used to shed light on the growth of SEI, with few multiscale approaches used to investigate the mechanism of lithium diffusion. The reason for this is that the interest in this transport phenomenon is relatively recent, and there are not enough data and information from experiments or from the electron/atom scale. For instance, kinetic Monte Carlo models require data and information from lower scale simulations such as DFT/AIMD. As an example, the kMC models used to study the growth of the SEI for times and lengths greater than the electron/atomic scale required data on the internal structure of the SEI and/or the activation energies of the various reaction from DFT/AIMD simulations [126,157,158]. The phase-field model is another valuable modeling approach capable of accurately describing and analyzing the behavior and evolution of complex interfaces between different phases or materials. This modeling technique has successfully explained distortions observed in experimental studies during the lithiation and delithiation processes of cathode material. Specifically, it has been employed to determine the diffusion velocity of lithium within a cathode material [144]. This modeling approach offers several advantages. Firstly, it may enable the study of diffusion a priori. Indeed, by examining different compounds and morphologies, researchers can gain valuable insights into the diffusion process. However, it is necessary to have knowledge of the diffusion of lithium in bulk conditions for each component of the SEI, which can be obtained from simplified systems using reactive atomistic simulations via well-trained MLFF. Furthermore, the phase-field model can be employed to extract the diffusion coefficient for each component of the SEI a posteriori by replicating experimental observations. In this case, a detailed spatial description of the different phases of the SEI is crucial to capture the diffusion behavior accurately. To achieve this, we suggest creating "in vitro" samples with well-defined and properly characterized SEI components and subjecting them to controlled experimental conditions. The transport of lithium ions within the crystal structures can be observed and analyzed by employing optical instrumentation. Subsequently, the phase-field modeling technique can be used to extract properties, i.e., the diffusion coefficient, which can serve as valuable inputs for continuum models.

This review delves into the transport phenomena of lithium within the SEI of batteries utilizing liquid electrolytes. However, it is crucial to emphasize that the discoveries and insights unveiled here can serve as valuable guidance for achieving a SEI with desired transport properties in future solid-state batteries (SSBs). In this direction, current studies have already been inspired by SEI in LIBs to design an artificial interface (in vitro) in SSBs with high ionic conductivity [134]. SSBs have gained significant relevance due to their notable benefits, including heightened safety features, improved energy density, extended cycle life, compatibility over a broader temperature range, suitability with high-energy materials, reduced internal resistance, and the potential for environmental benefits [159,160]. Promising avenues for SSBs development encompass quasisolid systems such as ionogels and polymer–glass composites, as well as solid oxide electrolytes. Quasisolid systems offer compelling platforms for fabricating SSBs by combining the advantages of both solid and liquid electrolytes [161]. The presence of liquid electrolytes within the solid matrix provides crucial high ionic conductivity, necessary for efficient ion transport in batteries. Solid oxide electrolytes find common application in high-temperature SSBs, enabling the utilization of high-energy-density electrode materials and enhancing overall battery performance [162]. In all of these quasisolid systems and solid oxide electrolytes, the formation and characteristics of the SEI play a pivotal role in determining the performance and stability of SSBs. In SSBs, similar to conventional LIBs, the SEI forms at the electrode–electrolyte interface

as a result of side electrolyte reduction reactions. However, the formation mechanisms and the composition of the SEI in SSBs may vary due to the distinct nature of the interface. For instance, in the quasisolid system, the presence of polymer or glass matrices alters the transport properties and ion diffusion kinetics, potentially affecting the reduction reactions of the electrolyte and thus influencing SEI formation [163]. On the other hand, SEI formation in SSBs with solid oxide electrolytes significantly differs from that in batteries with liquid electrolytes, mainly due to the distinct chemical and electrochemical properties of these electrolytes. In this case, the SEI layer typically forms through the interaction between lithium ions in the electrolyte and the oxide surface of the solid electrolyte [164]. Understanding and controlling the SEI formation in these systems is crucial to achieve efficient ion transport, stable electrode–electrolyte interfaces, and long-term cycling stability in SSBs [165,166].

5. Conclusions

Investigating the transport phenomena of lithium ions within the SEI of LIBs is crucial for understanding the formation and growth of SEI and its impact on the performance and durability of batteries. Although several studies have examined the influence of SEI on LIBs, relatively few have focused on determining the transport properties of SEI. Modeling this mechanism is challenging, as it occurs at different length and time scales and involves various modeling limitations.

In this review, we summarize the current computational efforts to comprehend the Li^+ diffusion inside the known SEI components of popular LIBs (see Figure 1). Electronic and atomistic scale models provide fairly accurate information on the diffusion mechanisms based on the structural and chemical characteristics of SEI components. Continuum models can predict the macroscopic behavior of lithium-ion transport within SEI and its impact on LIBs performance, whereas mesoscale modeling links small-scale models with large-scale models to properly understand this transport phenomenon. Despite progress, obstacles remain to shed light on lithium-ion diffusion within SEI, which are also related to the difficulty of obtaining experimental data and information.

In conclusion, in order to address these challenges and properly analyze this transport phenomenon, an intense collaboration between modeling and experimental approaches as well as a larger research effort on multiscale modeling are required. Indeed, this literature review has highlighted three critical aspects: the challenge of modeling a realistic SEI, the absence of models capable of effectively coupling different scales, and the difficulty of obtaining experimental observables to validate the models. To bridge these gaps and enhance the theoretical understanding of lithium transport in the SEI, we propose several favorable directions. At the lowest scale, we advocate the use of machine learning force fields, trained by accurate DFT simulations, to simulate the SEI formation and identify electrolyte degradation products. Considering that the SEI growth occurs over longer temporal and spatial scales compared to its initial formation, a statistical approach can be employed to effectively scale up the modeling. For example, we suggest De Angelis et al.'s [154] code that involves statistically positioning the inorganic components obtained from previous electrolyte degradation simulations to build a SEI of desired thickness. Such approach can provide crucial information for mesoscale and continuum models. For instance, once a SEI with composition and morphology as realistic as possible is known, the diffusion process of lithium within it could be sampled through kMC simulations. Furthermore, it is worthy to advance experimental techniques for evaluating the transport properties within the SEI. Therefore, we propose employing optical instrumentation to observe lithium transport in "in vitro" realized SEI components. By combining theoretical prediction with experimental observations, a deeper understanding of the transport properties calculated within the SEI can be achieved. Finally, given the increasing importance of solid-state batteries, we offer a concise overview of the SEI formation in these batteries. It is worth highlighting that the insights uncovered in this study can provide valuable guidance in achieving the desired transport properties of the SEI in future SSBs.

In our vision the proposed approaches, including the machine learning force field, statistical construction of the SEI, kinetic Monte Carlo simulations, and optical instrumentation, offer promising avenues for future research, leading to improved models and a better grasp of lithium-ion transport within SEI.

Author Contributions: R.C. contributed to this work by conducting a literature screening and investigation process and by writing the original draft. P.D.A. reviewed and edited this work and he verified the final considerations and perspectives. M.F., E.C. and P.A. supervised the research. E.C. and P.A. acquired the financial support for the project leading to this publication. All authors have read and agreed to the published version of the manuscript.

Funding: This research was funded by Battery Interface Genome–Materials Acceleration Platform project, grant number 957189.

Data Availability Statement: No data are associated to this work.

Acknowledgments: The authors acknowledge the support from the BIG-MAP, funded by the European Union's Horizon 2020 Research and Innovation Program under Grant Agreement No. 957189. The authors also acknowledge the computational resources provided by CINECA, PRACE and HPC@POLITO (http://www.hpc.polito.it (accessed on 1 November 2020)).

Conflicts of Interest: The authors declare no conflicts of interest

References

1. Kato, Y.; Ogumi, Z.; Martín, J.M.P. (Eds.) *Lithium-Ion Batteries: Overview, Simulation, and Diagnostics*; Pan Stanford Publishing: Singapore, 2019. [CrossRef]
2. Pistoia, G., Ed. *Lithium-Ion Batteries: Advances and Applications*, 1st ed.; Elsevier: Amsterdam, The Netherlands, 2014. [CrossRef]
3. Hannan, M.; Hoque, M.M.; Mohamed, A.; Ayob, A. Review of energy storage systems for electric vehicle applications: Issues and challenges. *Renew. Sustain. Energy Rev.* **2017**, *69*, 771–789. [CrossRef]
4. Dinger, A.; Martin, R.; Mosquet, X.; Rabl, M.; Rizoulis, D.; Russo, M.; Sticher, G. Batteries for electric cars: Challenges, opportunities, and the outlook to 2020. *Boston Consult. Group* **2010**, *7*, 2017.
5. De Angelis, P.; Tuninetti, M.; Bergamasco, L.; Calianno, L.; Asinari, P.; Laio, F.; Fasano, M. Data-driven appraisal of renewable energy potentials for sustainable freshwater production in Africa. *Renew. Sustain. Energy Rev.* **2021**, *149*, 111414. [CrossRef]
6. Dunn, B.; Kamath, H.; Tarascon, J.M. Electrical energy storage for the grid: A battery of choices. *Science* **2011**, *334*, 928–935. [CrossRef]
7. Eftekhari, A., Ed. *Future Lithium-Ion Batteries*; The Royal Society of Chemistry: London, UK, 2019. [CrossRef]
8. Amici, J.; Asinari, P.; Ayerbe, E.; Barboux, P.; Bayle-Guillemaud, P.; Behm, R.J.; Berecibar, M.; Berg, E.; Bhowmik, A.; Bodoardo, S.; et al. A roadmap for transforming research to invent the batteries of the future designed within the European large scale research initiative BATTERY 2030+. *Adv. Energy Mater.* **2022**, *12*, 2102785. [CrossRef]
9. Tarascon, J.M.; Armand, M. Issues and challenges facing rechargeable lithium batteries. *Nature* **2001**, *414*, 359–367. [CrossRef]
10. Xu, K. Nonaqueous liquid electrolytes for lithium-based rechargeable batteries. *Chem. Rev.* **2004**, *104*, 4303–4418. [CrossRef] [PubMed]
11. Latz, A.; Zausch, J. Thermodynamic consistent transport theory of Li-ion batteries. *J. Power Sources* **2011**, *196*, 3296–3302. [CrossRef]
12. Latz, A.; Zausch, J. Thermodynamic derivation of a Butler–Volmer model for intercalation in Li-ion batteries. *Electrochim. Acta* **2013**, *110*, 358–362. [CrossRef]
13. Xie, J.; Lu, Y.C. A retrospective on lithium-ion batteries. *Nat. Commun.* **2020**, *11*, 1–4. [CrossRef]
14. Goodenough, J.B.; Kim, Y. Challenges for rechargeable Li batteries. *Chem. Mater.* **2010**, *22*, 587–603. [CrossRef]
15. Li, F.; Bashir, S.; Liu, J.L. Nanostructured Materials for Next-Generation Energy Storage and Conversion. *Fuel Cells* **2018**. [CrossRef]
16. Xu, X.; Li, F.; Zhang, D.; Ji, S.; Huo, Y.; Liu, J. Facile construction of CoSn/Co3Sn2@ C nanocages as anode for superior lithium-/sodium-ion storage. *Carbon Neutralization* **2023**, *2*, 54–62. [CrossRef]
17. Yang, T.; Fan, W.; Wang, C.; Lei, Q.; Ma, Z.; Yu, L.; Zuo, X.; Nan, J. 2,3,4,5,6-Pentafluorophenyl methanesulfonate as a versatile electrolyte additive matches LiNi0.5Co0.2Mn0.3O2/graphite batteries working in a wide-temperature range. *ACS Appl. Mater. Interfaces* **2018**, *10*, 31735–31744. [CrossRef]
18. Wang, C.; Yu, L.; Fan, W.; Liu, J.; Ouyang, L.; Yang, L.; Zhu, M. Lithium difluorophosphate as a promising electrolyte lithium additive for high-voltage lithium-ion batteries. *ACS Appl. Energy Mater.* **2018**, *1*, 2647–2656. [CrossRef]
19. Jiang, Y.; Wu, Y.; Rui, X.; Peng, Y.; Xu, X.; Li, J.; Zhang, S.; Feng, X. In Situ Inorganic-Rich Electrode–Electrolyte Interphases for Safer 4.5 V Gr|| NCM811 Batteries Enabled by an Ethylene Carbonate-Free Electrolyte. *ACS Appl. Energy Mater.* **2022**, *5*, 11748–11755. [CrossRef]

20. Schultz, C.; Vedder, S.; Winter, M.; Nowak, S. Investigation of the decomposition of organic solvent-based lithium ion battery electrolytes with liquid chromatography-mass spectrometry. *Spectrosc. Eur* **2016**, *28*, 21–24.
21. Aurbach, D.; Markovsky, B.; Levi, M.; Levi, E.; Schechter, A.; Moshkovich, M.; Cohen, Y. New insights into the interactions between electrode materials and electrolyte solutions for advanced nonaqueous batteries. *J. Power Sources* **1999**, *81*, 95–111. [CrossRef]
22. Aurbach, D. Review of selected electrode–solution interactions which determine the performance of Li and Li ion batteries. *J. Power Sources* **2000**, *89*, 206–218. [CrossRef]
23. Yao, Y.X.; Yan, C.; Zhang, Q. Emerging interfacial chemistry of graphite anodes in lithium-ion batteries. *Chem. Commun.* **2020**, *56*, 14570–14584. [CrossRef]
24. Vetter, J.; Novák, P.; Wagner, M.R.; Veit, C.; Möller, K.C.; Besenhard, J.; Winter, M.; Wohlfahrt-Mehrens, M.; Vogler, C.; Hammouche, A. Ageing mechanisms in lithium-ion batteries. *J. Power Sources* **2005**, *147*, 269–281. [CrossRef]
25. Pastor-Fernández, C.; Yu, T.F.; Widanage, W.D.; Marco, J. Critical review of non-invasive diagnosis techniques for quantification of degradation modes in lithium-ion batteries. *Renew. Sustain. Energy Rev.* **2019**, *109*, 138–159. [CrossRef]
26. Reniers, J.M.; Mulder, G.; Howey, D.A. Review and performance comparison of mechanical-chemical degradation models for lithium-ion batteries. *J. Electrochem. Soc.* **2019**, *166*, A3189. [CrossRef]
27. Pinson, M.B.; Bazant, M.Z. Theory of SEI formation in rechargeable batteries: Capacity fade, accelerated aging and lifetime prediction. *J. Electrochem. Soc.* **2012**, *160*, A243. [CrossRef]
28. Gauthier, M.; Carney, T.J.; Grimaud, A.; Giordano, L.; Pour, N.; Chang, H.H.; Fenning, D.P.; Lux, S.F.; Paschos, O.; Bauer, C.; et al. Electrode–electrolyte interface in Li-ion batteries: Current understanding and new insights. *J. Phys. Chem. Lett.* **2015**, *6*, 4653–4672. [CrossRef]
29. An, S.J.; Li, J.; Daniel, C.; Mohanty, D.; Nagpure, S.; Wood III, D.L. The state of understanding of the lithium-ion-battery graphite solid electrolyte interphase (SEI) and its relationship to formation cycling. *Carbon* **2016**, *105*, 52–76. [CrossRef]
30. Kim, J.; Chae, O.B.; Lucht, B.L. Perspective—structure and stability of the solid electrolyte interphase on silicon anodes of lithium-ion batteries. *J. Electrochem. Soc.* **2021**, *168*, 030521. [CrossRef]
31. Rago, N.D.; Bareno, J.; Li, J.; Du, Z.; Wood III, D.L.; Steele, L.A.; Lamb, J.; Spangler, S.; Grosso, C.; Fenton, K.; et al. Effect of overcharge on Li (Ni0.5Mn0.3Co0.2) O2/Graphite lithium ion cells with poly (vinylidene fluoride) binder. I-Microstructural changes in the anode. *J. Power Sources* **2018**, *385*, 148–155. [CrossRef]
32. Wang, A.; Kadam, S.; Li, H.; Shi, S.; Qi, Y. Review on modeling of the anode solid electrolyte interphase (SEI) for lithium-ion batteries. *Npj Comput. Mater.* **2018**, *4*, 1–26. [CrossRef]
33. Malmgren, S.; Ciosek, K.; Hahlin, M.; Gustafsson, T.; Gorgoi, M.; Rensmo, H.; Edström, K. Comparing anode and cathode electrode/electrolyte interface composition and morphology using soft and hard X-ray photoelectron spectroscopy. *Electrochim. Acta* **2013**, *97*, 23–32. [CrossRef]
34. Peled, E. The electrochemical behavior of alkali and alkaline earth metals in nonaqueous battery systems—The solid electrolyte interphase model. *J. Electrochem. Soc.* **1979**, *126*, 2047. [CrossRef]
35. Peled, E.; Golodnitsky, D.; Ardel, G. Advanced model for solid electrolyte interphase electrodes in liquid and polymer electrolytes. *J. Electrochem. Soc.* **1997**, *144*, L208. [CrossRef]
36. Villevieille, C. Interfaces and Interphases in Batteries: How to Identify and Monitor Them Properly Using Surface Sensitive Characterization Techniques. *Adv. Mater. Interfaces* **2022**, *9*, 2101865. [CrossRef]
37. Wang, Y.; Nakamura, S.; Ue, M.; Balbuena, P.B. Theoretical studies to understand surface chemistry on carbon anodes for lithium-ion batteries: Reduction mechanisms of ethylene carbonate. *J. Am. Chem. Soc.* **2001**, *123*, 11708–11718. [CrossRef] [PubMed]
38. Leung, K. Electronic structure modeling of electrochemical reactions at electrode/electrolyte interfaces in lithium ion batteries. *J. Phys. Chem.* **2013**, *117*, 1539–1547. [CrossRef]
39. Aurbach, D.; Zaban, A.; Ein-Eli, Y.; Weissman, I.; Chusid, O.; Markovsky, B.; Levi, M.; Levi, E.; Schechter, A.; Granot, E. Recent studies on the correlation between surface chemistry, morphology, three-dimensional structures and performance of Li and Li-C intercalation anodes in several important electrolyte systems. *J. Power Sources* **1997**, *68*, 91–98. [CrossRef]
40. Schroder, K.W.; Celio, H.; Webb, L.J.; Stevenson, K.J. Examining solid electrolyte interphase formation on crystalline silicon electrodes: Influence of electrochemical preparation and ambient exposure conditions. *J. Phys. Chem. C* **2012**, *116*, 19737–19747. [CrossRef]
41. Yun, K.S.; Pai, S.J.; Yeo, B.C.; Lee, K.R.; Kim, S.J.; Han, S.S. Simulation protocol for prediction of a solid-electrolyte interphase on the silicon-based anodes of a lithium-ion battery: ReaxFF reactive force field. *J. Phys. Chem. Lett.* **2017**, *8*, 2812–2818. [CrossRef]
42. Lu, P.; Li, C.; Schneider, E.W.; Harris, S.J. Chemistry, impedance, and morphology evolution in solid electrolyte interphase films during formation in lithium ion batteries. *J. Phys. Chem. C* **2014**, *118*, 896–903. [CrossRef]
43. Winter, M. The solid electrolyte interphase–the most important and the least understood solid electrolyte in rechargeable Li batteries. *Z. für Phys. Chem.* **2009**, *223*, 1395–1406. [CrossRef]
44. Meda, U.S.; Lal, L.; Sushantha, M.; Garg, P. Solid Electrolyte Interphase (SEI), a boon or a bane for lithium batteries: A review on the recent advances. *J. Energy Storage* **2021**, 47, 103564. . [CrossRef]
45. An, S.J.; Li, J.; Du, Z.; Daniel, C.; Wood III, D.L. Fast formation cycling for lithium ion batteries. *J. Power Sources* **2017**, *342*, 846–852. [CrossRef]

46. Wood, D.L.; Li, J.; An, S.J. Formation challenges of lithium-ion battery manufacturing. *Joule* **2019**, *3*, 2884–2888. [CrossRef]
47. Shi, S.; Lu, P.; Liu, Z.; Qi, Y.; Hector Jr, L.G.; Li, H.; Harris, S.J. Direct calculation of Li-ion transport in the solid electrolyte interphase. *J. Am. Chem. Soc.* **2012**, *134*, 15476–15487. [CrossRef]
48. Ahmad, Z.; Venturi, V.; Hafiz, H.; Viswanathan, V. Interfaces in solid electrolyte interphase: Implications for lithium-ion batteries. *J. Phys. Chem. C* **2021**, *125*, 11301–11309. [CrossRef]
49. Chattopadhyay, S.; Lipson, A.L.; Karmel, H.J.; Emery, J.D.; Fister, T.T.; Fenter, P.A.; Hersam, M.C.; Bedzyk, M.J. In situ X-ray study of the solid electrolyte interphase (SEI) formation on graphene as a model Li-ion battery anode. *Chem. Mater.* **2012**, *24*, 3038–3043. [CrossRef]
50. Seidl, L.; Martens, S.; Ma, J.; Stimming, U.; Schneider, O. In situ scanning tunneling microscopy studies of the SEI formation on graphite electrodes for Li+-ion batteries. *Nanoscale* **2016**, *8*, 14004–14014. [CrossRef] [PubMed]
51. Li, Y.; Li, Y.; Pei, A.; Yan, K.; Sun, Y.; Wu, C.L.; Joubert, L.M.; Chin, R.; Koh, A.L.; Yu, Y.; et al. Atomic structure of sensitive battery materials and interfaces revealed by cryo–electron microscopy. *Science* **2017**, *358*, 506–510. [CrossRef]
52. Shinagawa, C.; Ushiyama, H.; Yamashita, K. Multiscale simulations for lithium-ion batteries: SEI film growth and capacity fading. *J. Electrochem. Soc.* **2017**, *164*, A3018. [CrossRef]
53. Horstmann, B.; Single, F.; Latz, A. Review on multi-scale models of solid-electrolyte interphase formation. *Curr. Opin. Electrochem.* **2019**, *13*, 61–69. [CrossRef]
54. Franco, A.A.; Rucci, A.; Brandell, D.; Frayret, C.; Gaberscek, M.; Jankowski, P.; Johansson, P. Boosting rechargeable batteries R&D by multiscale modeling: Myth or reality? *Chem. Rev.* **2019**, *119*, 4569–4627. [CrossRef]
55. Fong, R.; Von Sacken, U.; Dahn, J.R. Studies of lithium intercalation into carbons using nonaqueous electrochemical cells. *J. Electrochem. Soc.* **1990**, *137*, 2009. [CrossRef]
56. Xu, K.; von Cresce, A.; Lee, U. Differentiating contributions to "ion transfer" barrier from interphasial resistance and Li+ desolvation at electrolyte/graphite interface. *Langmuir* **2010**, *26*, 11538–11543. [CrossRef]
57. Single, F.; Horstmann, B.; Latz, A. Dynamics and morphology of solid electrolyte interphase (SEI). *Phys. Chem. Chem. Phys.* **2016**, *18*, 17810–17814. [CrossRef] [PubMed]
58. von Kolzenberg, L.; Latz, A.; Horstmann, B. Solid–electrolyte interphase during battery cycling: Theory of growth regimes. *ChemSusChem* **2020**, *13*, 3901–3910. [CrossRef] [PubMed]
59. Van der Ven, A.; Bhattacharya, J.; Belak, A.A. Understanding Li diffusion in Li-intercalation compounds. *Accounts Chem. Res.* **2013**, *46*, 1216–1225. [CrossRef]
60. Bedrov, D.; Borodin, O.; Hooper, J.B. Li+ transport and mechanical properties of model solid electrolyte interphases (SEI): insight from atomistic molecular dynamics simulations. *J. Phys. Chem. C* **2017**, *121*, 16098–16109. [CrossRef]
61. Moosbauer, D.; Zugmann, S.; Amereller, M.; Gores, H.J. Effect of ionic liquids as additives on lithium electrolytes: Conductivity, electrochemical stability, and aluminum corrosion. *J. Chem. Eng. Data* **2010**, *55*, 1794–1798. [CrossRef]
62. Adenusi, H.; Chass, G.A.; Passerini, S.; Tian, K.V.; Chen, G. Lithium Batteries and the Solid Electrolyte Interphase (SEI)—Progress and Outlook. *Adv. Energy Mater.* **2023**, *13*, 2203307. [CrossRef]
63. Soto, F.A.; Marzouk, A.; El-Mellouhi, F.; Balbuena, P.B. Understanding ionic diffusion through SEI components for lithium-ion and sodium-ion batteries: Insights from first-principles calculations. *Chem. Mater.* **2018**, *30*, 3315–3322. [CrossRef]
64. Ma, X.X.; Shen, X.; Chen, X.; Fu, Z.H.; Yao, N.; Zhang, R.; Zhang, Q. The Origin of Fast Lithium-Ion Transport in the Inorganic Solid Electrolyte Interphase on Lithium Metal Anodes. *Small Struct.* **2022**, *3*, 2200071. [CrossRef]
65. Shi, S.; Qi, Y.; Li, H.; Hector Jr, L.G. Defect thermodynamics and diffusion mechanisms in Li2CO3 and implications for the solid electrolyte interphase in Li-ion batteries. *J. Phys. Chem. C* **2013**, *117*, 8579–8593. [CrossRef]
66. Alzate-Vargas, L.; Vikrant, K.; Allu, S.; Fattebert, J.L. Atomistic modeling of LiF microstructure ionic conductivity and its influence on nucleation and plating. *Phys. Rev. Mater.* **2022**, *6*, 095402. [CrossRef]
67. Benitez, L.; Seminario, J.M. Ion diffusivity through the solid electrolyte interphase in lithium-ion batteries. *J. Electrochem. Soc.* **2017**, *164*, E3159. [CrossRef]
68. Safari, M.; Morcrette, M.; Teyssot, A.; Delacourt, C. Multimodal physics-based aging model for life prediction of Li-ion batteries. *J. Electrochem. Soc.* **2008**, *156*, A145. [CrossRef]
69. Santhanagopalan, S.; Guo, Q.; Ramadass, P.; White, R.E. Review of models for predicting the cycling performance of lithium ion batteries. *J. Power Sources* **2006**, *156*, 620–628. [CrossRef]
70. Ning, G.; Popov, B.N. Cycle life modeling of lithium-ion batteries. *J. Electrochem. Soc.* **2004**, *151*, A1584. [CrossRef]
71. Maier, J. *Physical Chemistry of Ionic Materials: Ions and Electrons in Solids*; John Wiley & Sons: Hoboken, NJ, USA, 2023.
72. Pan, J.; Cheng, Y.T.; Qi, Y. General method to predict voltage-dependent ionic conduction in a solid electrolyte coating on electrodes. *Phys. Rev. B* **2015**, *91*, 134116. [CrossRef]
73. Pan, J.; Zhang, Q.; Xiao, X.; Cheng, Y.T.; Qi, Y. Design of nanostructured heterogeneous solid ionic coatings through a multiscale defect model. *ACS Appl. Mater. Interfaces* **2016**, *8*, 5687–5693. [CrossRef]
74. Iddir, H.; Curtiss, L.A. Li ion diffusion mechanisms in bulk monoclinic Li2CO3 crystals from density functional studies. *J. Phys. Chem. C* **2010**, *114*, 20903–20906. [CrossRef]
75. Kohn, W.; Sham, L.J. Self-consistent equations including exchange and correlation effects. *Phys. Rev.* **1965**, *140*, A1133. [CrossRef]
76. Nazri, G.; Muller, R.H. Composition of surface layers on Li electrodes in PC, LiClO4 of very low water content. *J. Electrochem. Soc.* **1985**, *132*, 2050. [CrossRef]

77. Jónsson, H.; Mills, G.; Jacobsen, K.W. Nudged elastic band method for finding minimum energy paths of transitions. In *Classical and Quantum Dynamics in Condensed Phase Simulations*; World Scientific: London, UK, 1998; pp. 385–404. [CrossRef]
78. Toyoura, K.; Koyama, Y.; Kuwabara, A.; Tanaka, I. Effects of off-stoichiometry of LiC6 on the lithium diffusion mechanism and diffusivity by first principles calculations. *J. Phys. Chem. C* **2010**, *114*, 2375–2379. [CrossRef]
79. Chen, Y.; Ouyang, C.; Song, L.; Sun, Z. Electrical and lithium ion dynamics in three main components of solid electrolyte interphase from density functional theory study. *J. Phys. Chem. C* **2011**, *115*, 7044–7049. [CrossRef]
80. Persson, K.; Sethuraman, V.A.; Hardwick, L.J.; Hinuma, Y.; Meng, Y.S.; Van Der Ven, A.; Srinivasan, V.; Kostecki, R.; Ceder, G. Lithium diffusion in graphitic carbon. *J. Phys. Chem. Lett.* **2010**, *1*, 1176–1180. [CrossRef]
81. Ramasubramanian, A.; Yurkiv, V.; Foroozan, T.; Ragone, M.; Shahbazian-Yassar, R.; Mashayek, F. Lithium diffusion mechanism through solid–electrolyte interphase in rechargeable lithium batteries. *J. Phys. Chem. C* **2019**, *123*, 10237–10245. [CrossRef]
82. Zheng, J.; Ju, Z.; Zhang, B.; Nai, J.; Liu, T.; Liu, Y.; Xie, Q.; Zhang, W.; Wang, Y.; Tao, X. Lithium ion diffusion mechanism on the inorganic components of the solid–electrolyte interphase. *J. Mater. Chem. A* **2021**, *9*, 10251–10259. [CrossRef]
83. Car, R.; Parrinello, M. Unified approach for molecular dynamics and density-functional theory. *Phys. Rev. Lett.* **1985**, *55*, 2471. [CrossRef]
84. Frenkel, D.; Smit, B. *Understanding Molecular Simulation: From Algorithms to Applications*; Elsevier: Amsterdam, The Netherlands, 2001; Volume 1. [CrossRef]
85. Satoh, A. *Introduction to Practice of Molecular Simulation: Molecular Dynamics, Monte Carlo, Brownian Dynamics, Lattice Boltzmann and Dissipative Particle Dynamics*; Elsevier: Amsterdam, The Netherlands, 2010. [CrossRef]
86. Allen, M.P.; Tildesley, D.J. *Computer Simulation of Liquids*, 2nd ed.; Oxford University Press: Oxford, UK, 2017. [CrossRef]
87. Senftle, T.P.; Hong, S.; Islam, M.M.; Kylasa, S.B.; Zheng, Y.; Shin, Y.K.; Junkermeier, C.; Engel-Herbert, R.; Janik, M.J.; Aktulga, H.M.; et al. The ReaxFF reactive force-field: Development, applications and future directions. *Npj Comput. Mater.* **2016**, *2*, 1–14. [CrossRef]
88. Harrison, J.A.; Schall, J.D.; Maskey, S.; Mikulski, P.T.; Knippenberg, M.T.; Morrow, B.H. Review of force fields and intermolecular potentials used in atomistic computational materials research. *Appl. Phys. Rev.* **2018**, *5*, 031104. [CrossRef]
89. Unke, O.T.; Chmiela, S.; Sauceda, H.E.; Gastegger, M.; Poltavsky, I.; Schütt, K.T.; Tkatchenko, A.; Muüller, K.R. Machine learning force fields. *Chem. Rev.* **2021**, *121*, 10142–10186. [CrossRef] [PubMed]
90. Pauling, L. The nature of the chemical bond. II. The one-electron bond and the three-electron bond. *J. Am. Chem. Soc.* **1931**, *53*, 3225–3237. [CrossRef]
91. Brenner, D.W. Empirical potential for hydrocarbons for use in simulating the chemical vapor deposition of diamond films. *Phys. Rev. B* **1990**, *42*, 9458. [CrossRef] [PubMed]
92. Stuart, S.J.; Tutein, A.B.; Harrison, J.A. A reactive potential for hydrocarbons with intermolecular interactions. *J. Chem. Phys.* **2000**, *112*, 6472–6486. [CrossRef]
93. Tersoff, J. New empirical approach for the structure and energy of covalent systems. *Phys. Rev. B* **1988**, *37*, 6991. [CrossRef] [PubMed]
94. Van Duin, A.C.; Dasgupta, S.; Lorant, F.; Goddard, W.A. ReaxFF: A reactive force field for hydrocarbons. *J. Phys. Chem. A* **2001**, *105*, 9396–9409. [CrossRef]
95. Jorgensen, W.L.; Maxwell, D.S.; Tirado-Rives, J. Development and testing of the OPLS all-atom force field on conformational energetics and properties of organic liquids. *J. Am. Chem. Soc.* **1996**, *118*, 11225–11236. [CrossRef]
96. Canongia Lopes, J.N.; Pádua, A.A. Molecular force field for ionic liquids composed of triflate or bistriflylimide anions. *J. Phys. Chem. B* **2004**, *108*, 16893–16898. [CrossRef]
97. Borodin, O.; Smith, G.D. Development of many- body polarizable force fields for Li-battery components: 1. Ether, Alkane, and carbonate-based solvents. *J. Phys. Chem. B* **2006**, *110*, 6279–6292. [CrossRef]
98. Borodin, O.; Smith, G.D.; Fan, P. Molecular dynamics simulations of lithium alkyl carbonates. *J. Phys. Chem. B* **2006**, *110*, 22773–22779. [CrossRef]
99. Starovoytov, O.N.; Borodin, O.; Bedrov, D.; Smith, G.D. Development of a polarizable force field for molecular dynamics simulations of poly (ethylene oxide) in aqueous solution. *J. Chem. Theory Comput.* **2011**, *7*, 1902–1915. [CrossRef] [PubMed]
100. Chiavazzo, E.; Fasano, M.; Asinari, P.; Decuzzi, P. Scaling behaviour for the water transport in nanoconfined geometries. *Nat. Commun.* **2014**, *5*, 1–11. [CrossRef]
101. Fasano, M.; Bevilacqua, A.; Chiavazzo, E.; Humplik, T.; Asinari, P. Mechanistic correlation between water infiltration and framework hydrophilicity in MFI zeolites. *Sci. Rep.* **2019**, *9*, 18429. [CrossRef]
102. Márquez, A.; Balbuena, P.B. Molecular dynamics study of Graphite/Electrolyte interfaces. *J. Electrochem. Soc.* **2001**, *148*, A624. [CrossRef]
103. Zhuang, G.V.; Xu, K.; Yang, H.; Jow, T.R.; Ross, P.N. Lithium ethylene dicarbonate identified as the primary product of chemical and electrochemical reduction of EC in 1.2 M LiPF6/EC: EMC electrolyte. *J. Phys. Chem. B* **2005**, *109*, 17567–17573. [CrossRef]
104. Nie, M.; Chalasani, D.; Abraham, D.P.; Chen, Y.; Bose, A.; Lucht, B.L. Lithium ion battery graphite solid electrolyte interphase revealed by microscopy and spectroscopy. *J. Phys. Chem. C* **2013**, *117*, 1257–1267. [CrossRef]
105. Borodin, O.; Zhuang, G.V.; Ross, P.N.; Xu, K. Molecular dynamics simulations and experimental study of lithium ion transport in dilithium ethylene dicarbonate. *J. Phys. Chem. C* **2013**, *117*, 7433–7444. [CrossRef]

106. Jow, T.R.; Marx, M.B.; Allen, J.L. Distinguishing Li+ charge transfer kinetics at NCA/electrolyte and graphite/electrolyte interfaces, and NCA/electrolyte and LFP/electrolyte interfaces in Li-ion cells. *J. Electrochem. Soc.* **2012**, *159*, A604. [CrossRef]
107. Jow, T.R.; Allen, J.; Marx, M.; Nechev, K.; Deveney, B.; Rickman, S. Electrolytes, SEI and charge discharge kinetics in Li-ion batteries. *ECS Trans.* **2010**, *25*, 3. [CrossRef]
108. Xu, K.; Lam, Y.; Zhang, S.S.; Jow, T.R.; Curtis, T.B. Solvation sheath of Li+ in nonaqueous electrolytes and its implication of graphite/electrolyte interface chemistry. *J. Phys. Chem. C* **2007**, *111*, 7411–7421. [CrossRef]
109. Borodin, O. Polarizable force field development and molecular dynamics simulations of ionic liquids. *J. Phys. Chem. B* **2009**, *113*, 11463–11478. [CrossRef]
110. Muralidharan, A.; Chaudhari, M.I.; Pratt, L.R.; Rempe, S.B. Molecular dynamics of lithium ion transport in a model solid electrolyte interphase. *Sci. Rep.* **2018**, *8*, 10736. [CrossRef] [PubMed]
111. Muralidharan, A.; Chaudhari, M.; Rempe, S.; Pratt, L.R. Molecular dynamics simulations of lithium ion transport through a model solid electrolyte interphase (sei) layer. *ECS Trans.* **2017**, *77*, 1155. [CrossRef]
112. Kim, S.Y.; Ostadhossein, A.; Van Duin, A.C.; Xiao, X.; Gao, H.; Qi, Y. Self-generated concentration and modulus gradient coating design to protect Si nano-wire electrodes during lithiation. *Phys. Chem. Chem. Phys.* **2016**, *18*, 3706–3715. [CrossRef] [PubMed]
113. Bedrov, D.; Smith, G.D.; van Duin, A.C. Reactions of singly-reduced ethylene carbonate in lithium battery electrolytes: A molecular dynamics simulation study using the ReaxFF. *J. Phys. Chem. A* **2012**, *116*, 2978–2985. [CrossRef]
114. Islam, M.M.; Van Duin, A.C. Reductive decomposition reactions of ethylene carbonate by explicit electron transfer from lithium: an eReaxFF molecular dynamics study. *J. Phys. Chem. C* **2016**, *120*, 27128–27134. [CrossRef]
115. Kim, S.P.; Van Duin, A.C.; Shenoy, V.B. Effect of electrolytes on the structure and evolution of the solid electrolyte interphase (SEI) in Li-ion batteries: A molecular dynamics study. *J. Power Sources* **2011**, *196*, 8590–8597. [CrossRef]
116. De Angelis, P. Reactive and Non-Reactive Interface Modelling for Energy Materials. Ph.D. Thesis, Politecnico di Torino, Torino, IT, USA, 2022.
117. Chenoweth, K.; Van Duin, A.C.; Goddard, W.A. ReaxFF reactive force field for molecular dynamics simulations of hydrocarbon oxidation. *J. Phys. Chem. A* **2008**, *112*, 1040–1053. [CrossRef]
118. Castro-Marcano, F.; Kamat, A.M.; Russo, M.F., Jr.; van Duin, A.C.; Mathews, J.P. Combustion of an Illinois No. 6 coal char simulated using an atomistic char representation and the ReaxFF reactive force field. *Combust. Flame* **2012**, *159*, 1272–1285. [CrossRef]
119. Strachan, A.; van Duin, A.C.; Chakraborty, D.; Dasgupta, S.; Goddard, W.A., III. Shock waves in high-energy materials: The initial chemical events in nitramine RDX. *Phys. Rev. Lett.* **2003**, *91*, 098301. [CrossRef]
120. Weismiller, M.R.; Van Duin, A.C.; Lee, J.; Yetter, R.A. ReaxFF reactive force field development and applications for molecular dynamics simulations of ammonia borane dehydrogenation and combustion. *J. Phys. Chem. A* **2010**, *114*, 5485–5492. [CrossRef] [PubMed]
121. Agrawalla, S.; Van Duin, A.C. Development and application of a ReaxFF reactive force field for hydrogen combustion. *J. Phys. Chem. A* **2011**, *115*, 960–972. [CrossRef] [PubMed]
122. Yang, M.; Bonati, L.; Polino, D.; Parrinello, M. Using metadynamics to build neural network potentials for reactive events: The case of urea decomposition in water. *Catal. Today* **2022**, *387*, 143–149. [CrossRef]
123. Andersen, M.; Panosetti, C.; Reuter, K. A practical guide to surface kinetic Monte Carlo simulations. *Front. Chem.* **2019**, *7*, 202. [CrossRef]
124. Methekar, R.N.; Northrop, P.W.; Chen, K.; Braatz, R.D.; Subramanian, V.R. Kinetic Monte Carlo simulation of surface heterogeneity in graphite anodes for lithium-ion batteries: Passive layer formation. *J. Electrochem. Soc.* **2011**, *158*, A363. [CrossRef]
125. Fitzgerald, M.; Picard, R.; Silver, R. Canonical transition probabilities for adaptive Metropolis simulation. *Europhys. Lett.* **1999**, *46*, 282. [CrossRef]
126. Esmaeilpour, M.; Jana, S.; Li, H.; Soleymanibrojeni, M.; Wenzel, W. A Solution-Mediated Pathway for the Growth of the Solid Electrolyte Interphase in Lithium-Ion Batteries. *Adv. Energy Mater.* **2023**, 2203966. [CrossRef]
127. Colclasure, A.M.; Smith, K.A.; Kee, R.J. Modeling detailed chemistry and transport for solid-electrolyte-interface (SEI) films in Li–ion batteries. *Electrochim. Acta* **2011**, *58*, 33–43. [CrossRef]
128. Christensen, J.; Newman, J. A mathematical model for the lithium-ion negative electrode solid electrolyte interphase. *J. Electrochem. Soc.* **2004**, *151*, A1977. [CrossRef]
129. Ning, G.; White, R.E.; Popov, B.N. A generalized cycle life model of rechargeable Li-ion batteries. *Electrochim. Acta* **2006**, *51*, 2012–2022. [CrossRef]
130. Doyle, M.; Fuller, T.F.; Newman, J. Modeling of galvanostatic charge and discharge of the lithium/polymer/insertion cell. *J. Electrochem. Soc.* **1993**, *140*, 1526. [CrossRef]
131. Ramadass, P.; Haran, B.; Gomadam, P.M.; White, R.; Popov, B.N. Development of first principles capacity fade model for Li-ion cells. *J. Electrochem. Soc.* **2004**, *151*, A196. [CrossRef]
132. Single, F.; Latz, A.; Horstmann, B. Identifying the mechanism of continued growth of the solid–electrolyte interphase. *ChemSusChem* **2018**, *11*, 1950–1955. [CrossRef]
133. Cheng, X.B.; Zhang, R.; Zhao, C.Z.; Wei, F.; Zhang, J.G.; Zhang, Q. A review of solid electrolyte interphases on lithium metal anode. *Adv. Sci.* **2016**, *3*, 1500213. [CrossRef] [PubMed]

134. Liu, Y.; Hu, R.; Zhang, D.; Liu, J.; Liu, F.; Cui, J.; Lin, Z.; Wu, J.; Zhu, M. Constructing Li-Rich Artificial SEI Layer in Alloy–Polymer Composite Electrolyte to Achieve High Ionic Conductivity for All-Solid-State Lithium Metal Batteries. *Adv. Mater.* **2021**, *33*, 2004711. [CrossRef]
135. Lowe, J.S.; Siegel, D.J. Modeling the interface between lithium metal and its native oxide. *ACS Appl. Mater. Interfaces* **2020**, *12*, 46015–46026. [CrossRef]
136. Lorger, S.; Usiskin, R.; Maier, J. Transport and charge carrier chemistry in lithium oxide. *J. Electrochem. Soc.* **2019**, *166*, A2215. [CrossRef]
137. Guo, R.; Gallant, B.M. Li2O solid electrolyte interphase: Probing transport properties at the chemical potential of lithium. *Chem. Mater.* **2020**, *32*, 5525–5533. [CrossRef]
138. Less, G.B.; Seo, J.H.; Han, S.; Sastry, A.M.; Zausch, J.; Latz, A.; Schmidt, S.; Wieser, C.; Kehrwald, D.; Fell, S. Micro-scale modeling of Li-ion batteries: Parameterization and validation. *J. Electrochem. Soc.* **2012**, *159*, A697. [CrossRef]
139. Bhowmik, A.; Castelli, I.E.; Garcia-Lastra, J.M.; Jørgensen, P.B.; Winther, O.; Vegge, T. A perspective on inverse design of battery interphases using multi-scale modelling, experiments and generative deep learning. *Energy Storage Mater.* **2019**, *21*, 446–456. [CrossRef]
140. Shi, S.; Gao, J.; Liu, Y.; Zhao, Y.; Wu, Q.; Ju, W.; Ouyang, C.; Xiao, R. Multi-scale computation methods: Their applications in lithium-ion battery research and development. *Chin. Phys. B* **2015**, *25*, 018212. [CrossRef]
141. Single, F.; Horstmann, B.; Latz, A. Revealing SEI morphology: In-depth analysis of a modeling approach. *J. Electrochem. Soc.* **2017**, *164*, E3132. [CrossRef]
142. Zeng, Z.; Liang, W.I.; Liao, H.G.; Xin, H.L.; Chu, Y.H.; Zheng, H. Visualization of electrode–electrolyte interfaces in LiPF6/EC/DEC electrolyte for lithium ion batteries via in situ TEM. *Nano Lett.* **2014**, *14*, 1745–1750. [CrossRef] [PubMed]
143. An, S.J.; Li, J.; Daniel, C.; Meyer III, H.M.; Trask, S.E.; Polzin, B.J.; Wood III, D.L. Electrolyte volume effects on electrochemical performance and solid electrolyte interphase in Si-graphite/NMC lithium-ion pouch cells. *ACS Appl. Mater. Interfaces* **2017**, *9*, 18799–18808. [CrossRef]
144. Merryweather, A.J.; Schnedermann, C.; Jacquet, Q.; Grey, C.P.; Rao, A. Operando optical tracking of single-particle ion dynamics in batteries. *Nature* **2021**, *594*, 522–528. [CrossRef]
145. Clark, S.; Bleken, F.L.; Stier, S.; Flores, E.; Andersen, C.W.; Marcinek, M.; Szczesna-Chrzan, A.; Gaberscek, M.; Palacin, M.R.; Uhrin, M.; et al. Toward a unified description of battery data. *Adv. Energy Mater.* **2022**, *12*, 2102702. [CrossRef]
146. Castelli, I.E.; Arismendi-Arrieta, D.J.; Bhowmik, A.; Cekic-Laskovic, I.; Clark, S.; Dominko, R.; Flores, E.; Flowers, J.; Ulvskov Frederiksen, K.; Friis, J.; et al. Data Management Plans: The Importance of Data Management in the BIG-MAP Project. *Batter. Supercaps* **2021**, *4*, 1803–1812. [CrossRef]
147. Wang, Y.; Liu, Y.; Tu, Y.; Wang, Q. Reductive decomposition of solvents and additives toward solid-electrolyte interphase formation in lithium-ion battery. *J. Phys. Chem. C* **2020**, *124*, 9099–9108. [CrossRef]
148. Joraleechanchai, N.; Duangdangchote, S.; Sawangphruk, M. Machine Learning and Reactive Force Field Molecular Dynamics Investigation of Electrolytes for Ultra-fast Charging Li-ion Batteries. *ECS Trans.* **2020**, *97*, 45. [CrossRef]
149. Barcaro, G.; Monti, S.; Sementa, L.; Carravetta, V. Parametrization of a reactive force field (ReaxFF) for molecular dynamics simulations of Si nanoparticles. *J. Chem. Theory Comput.* **2017**, *13*, 3854–3861. [CrossRef]
150. Yao, N.; Chen, X.; Fu, Z.H.; Zhang, Q. Applying classical, ab initio, and machine-learning molecular dynamics simulations to the liquid electrolyte for rechargeable batteries. *Chem. Rev.* **2022**, *122*, 10970–11021. [CrossRef]
151. Deringer, V.L. Modelling and understanding battery materials with machine-learning-driven atomistic simulations. *J. Phys. Energy* **2020**, *2*, 041003. [CrossRef]
152. Lombardo, T.; Hoock, J.B.; Primo, E.N.; Ngandjong, A.C.; Duquesnoy, M.; Franco, A.A. Accelerated optimization methods for force-field parametrization in battery electrode manufacturing modeling. *Batter. Supercaps* **2020**, *3*, 721–730. [CrossRef]
153. Chmiela, S.; Tkatchenko, A.; Sauceda, H.E.; Poltavsky, I.; Schütt, K.T.; Müller, K.R. Machine learning of accurate energy-conserving molecular force fields. *Sci. Adv.* **2017**, *3*, e1603015. [CrossRef]
154. De Angelis, P.; Cappabianca, R.; Asinari, P.; Chiavazzo, E. SEI Builder-Jupyter notebooks to build inital SEI morphology. *Zenodo* **2022**. [CrossRef]
155. Edge, J.S.; O'Kane, S.; Prosser, R.; Kirkaldy, N.D.; Patel, A.N.; Hales, A.; Ghosh, A.; Ai, W.; Chen, J.; Yang, J.; et al. Lithium ion battery degradation: What you need to know. *Phys. Chem. Chem. Phys.* **2021**, *23*, 8200–8221. [CrossRef] [PubMed]
156. Guan, P.; Liu, L.; Lin, X. Simulation and experiment on solid electrolyte interphase (SEI) morphology evolution and lithium-ion diffusion. *J. Electrochem. Soc.* **2015**, *162*, A1798. [CrossRef]
157. Abbott, J.W.; Hanke, F. Kinetically Corrected Monte Carlo–Molecular Dynamics Simulations of Solid Electrolyte Interphase Growth. *J. Chem. Theory Comput.* **2022**, *18*, 925–934. [CrossRef]
158. Gerasimov, M.; Soto, F.A.; Wagner, J.; Baakes, F.; Guo, N.; Ospina-Acevedo, F.; Roder, F.; Balbuena, P.B.; Krewer, U. Species Distribution During Solid Electrolyte Interphase Formation on Lithium Using MD/DFT-Parameterized Kinetic Monte Carlo Simulations. *J. Phys. Chem. C* **2023**. [CrossRef]
159. Kim, J.G.; Son, B.; Mukherjee, S.; Schuppert, N.; Bates, A.; Kwon, O.; Choi, M.J.; Chung, H.Y.; Park, S. A review of lithium and non-lithium based solid state batteries. *J. Power Sources* **2015**, *282*, 299–322. [CrossRef]
160. Lee, D.; Lee, H.; Song, T.; Paik, U. Toward High Rate Performance Solid-State Batteries. *Adv. Energy Mater.* **2022**, *12*, 2200948. [CrossRef]

161. Zhai, Y.; Yang, G.; Zeng, Z.; Song, S.; Li, S.; Hu, N.; Tang, W.; Wen, Z.; Lu, L.; Molenda, J. Composite hybrid quasi-solid electrolyte for high-energy lithium metal batteries. *ACS Appl. Energy Mater.* **2021**, *4*, 7973–7982. [CrossRef]
162. Miara, L.; Windmüller, A.; Tsai, C.L.; Richards, W.D.; Ma, Q.; Uhlenbruck, S.; Guillon, O.; Ceder, G. About the compatibility between high voltage spinel cathode materials and solid oxide electrolytes as a function of temperature. *ACS Appl. Mater. Interfaces* **2016**, *8*, 26842–26850. [CrossRef] [PubMed]
163. Shi, Y.; Wan, J.; Liu, G.X.; Zuo, T.T.; Song, Y.X.; Liu, B.; Guo, Y.G.; Wen, R.; Wan, L.J. Interfacial Evolution of Lithium Dendrites and Their Solid Electrolyte Interphase Shells of Quasi-Solid-State Lithium-Metal Batteries. *Angew. Chem. Int. Ed.* **2020**, *59*, 18120–18125. [CrossRef] [PubMed]
164. Thangadurai, V.; Weppner, W. Recent progress in solid oxide and lithium ion conducting electrolytes research. *Ionics* **2006**, *12*, 81–92. [CrossRef]
165. Wu, L.T.; Nachimuthu, S.; Brandell, D.; Jiang, J.C. Prediction of SEI Formation in All-Solid-State Batteries: Computational Insights from PCL-based Polymer Electrolyte Decomposition on Lithium-Metal. *Batter. Supercaps* **2022**, *5*, e202200088. [CrossRef]
166. Wu, B.; Wang, S.; Lochala, J.; Desrochers, D.; Liu, B.; Zhang, W.; Yang, J.; Xiao, J. The role of the solid electrolyte interphase layer in preventing Li dendrite growth in solid-state batteries. *Energy Environ. Sci.* **2018**, *11*, 1803–1810. [CrossRef]